Preprints.org

Review

Not peer-reviewed version

The Application of Textile Materials in the Interfacial Solar Steam Generation for Water Purification and Desalination: A Review

HAROON ABDELRAHMAN MOHAMED SAEED , Veronica Valerian Kazimoto , Weilin Xu , Hongjun Yang *

Posted Date: 28 December 2023

doi: 10.20944/preprints202312.2214.v1

Keywords: interfacial solar steam generation; textile materials; wastewater purification; desalination; woven fabric; electro-spun membranes

Preprints.org is a free multidiscipline platform providing preprint service that is dedicated to making early versions of research outputs permanently available and citable. Preprints posted at Preprints.org appear in Web of Science, Crossref, Google Scholar, Scilit, Europe PMC.

Copyright: This is an open access article distributed under the Creative Commons Attribution License which permits unrestricted use, distribution, and reproduction in any medium, provided the original work is properly cited.

Preprints (www.preprints.org) | NOT PEER-REVIEWED | Posted: 28 December 2023 doi:10.20944/preprints202312.2214.v1

Disclaimer/Publisher's Note: The statements, opinions, and data contained in all publications are solely those of the individual author(s) and contributor(s) and not of MDPI and/or the editor(s). MDPI and/or the editor(s) disclaim responsibility for any injury to people or property resulting from any ideas, methods, instructions, or products referred to in the content.

Review

The Application of Textile Materials in the Interfacial Solar Steam Generation for Water Purification and Desalination: A Review

Haroon A. M. Saeed [1,2], Veronica Valerian Kazimoto [3], Willin Xu [1] and Hongjun Yang [1,*]

[1] Key Laboratory of Green Processing and Functional New Textile Materials of Ministry of Education, Wuhan Textile University, Wuhan 430200, P. R. China; h_j.yang@yahoo.com; weilin_xu@hotmail.com
[2] Textile Engineering Department, Faculty of Industries Engineering &Technology, University of Gezira, Wad Madani, P.O Box 20, Sudan; haroonsaeed75@gmail.com
[3] College of Textile, Wuhan Textile University, Wuhan, Hubei Province 430200, People's Republic of China; veronicavalerian123@gmail.com
* Correspondence: h_j.yang@yahoo.com; Tel./Fax: +86-27-59367690

Abstract: The global increase in population, the phenomenon of climate change, the issue of water pollution and contamination, and the inadequate management of water resources all exert heightened strain on freshwater reserves. The potential utilization of the interfacial solar steam generation (ISSG) system, which utilizes photothermal conversion to generate heat on material surfaces for wastewater purification and desalination purposes, has been successfully demonstrated. Textile materials based ISSG devices, including (woven, nonwoven and knitting) fabrics and electrospinning membranes, exhibit distinct properties such as rough surface texture, high porosity, significant surface area, exceptional flexibility, and robust mechanical strength. These characteristics, combined with their affordability, accessibility, and economic viability for widespread implementation, make them extremely attractive for applications in SSG. In this review, a comprehensive analysis of emerging concepts, advancements and applications of textile materials (woven, nonwoven, and knitting) fabrics and electro-spun membranes in the ISSG for wastewater purification and desalination is highlighted. We also emphasize significant obstacles and potential prospects in both theoretical investigations and real-world implementations, aiming to contribute to future advancements in the domain of textile based materials interfacial evaporation in wastewater purification and desalination. Furthermore, the drawbacks and the challenges of ISSG systems are also highlighted.

Keywords: interfacial solar steam generation; textile materials; wastewater purification; desalination; woven fabric; electro-spun membranes

1. Introduction:

Although approximately 75% of the surface area of Earth is covered by seawater [1–3]. However, almost 97% of the Earth's water is saline, meaning it has a high concentration of dissolved salts [4–7]. This saline water is primarily found in the oceans and seas, making it mostly unsuitable for direct utilization in most applications, including drinking, irrigation, and industrial processes [8,9] this leading to a significant proportion exceeding one-third of the global populace resides within nations confronting water scarcity [10,11]. And it is expected that this proportion will increase to around two-thirds by the year 2025 [12–14]. Based on the United Nations World Water Development Report 2019, it is evident that global human water consumption has escalated to six times its level a century ago. Furthermore, projections indicate this demand will surge from 20% to 50% by 2050 [15,16]. However, the global subject of freshwater scarcity has been identified as a significant issue [17]. The scarcity of easily accessible drinking water is increasingly posing a significant issue for the advancement and sustainability of functional civilizations [18] due to the climate change [3,19], socio-economic [20,21], rapid growth of urbanization [22] and industrialization [6,23–25] agriculture and animal husbandry

© 2023 by the author(s). Distributed under a Creative Commons CC BY license.

Preprints (www.preprints.org) | NOT PEER-REVIEWED | Posted: 28 December 2023 doi:10.20944/preprints202312.2214.v1

[26,27], expansion of the population [28,29] and the escalating levels of water pollution [30,31]. Providing clean drinking water globally is widely recognized as a fundamental requirement for promoting optimal human health. However, it is reported that; the daily water intake necessary for individuals to sustain various physiological processes typically ranges from 2.5 to 7.5 liters. Despite the tremendous advancements in technological development, providing a secure and environmentally friendly water supply continues to pose significant challenges, particularly in emerging nations and geographically isolated regions [32]. However, addressing the scarcity of freshwater requires a multi-faceted approach. It involves implementing sustainable water management practices, promoting water conservation, investing in infrastructure for water storage and distribution, improving water quality through pollution control measures, and developing innovative technologies for wastewater purification and desalination.

Currently, there are multiple techniques for the desalination of seawater, including membrane distillation [33], reverse osmosis [9,10,19], multistage flash (MSF) technology [31], electrodialysis [34], and solar-driven evaporation [13,17]. However, using industrial desalination techniques and wastewater purification is constrained by protracted operations, costly devices, and significant power usage [35]. Solar energy is considered one of the most environmentally friendly, among other sources such as wind energy, tidal energy, and geothermal energy [6,36]. However, recently, interfacial solar steam generation (ISSG) has garnered significant interest and is widely regarded as a promising method for producing pure water in academic and industrial settings [37,38]. This is due to its cost-effectiveness [36,39], low energy usage, the cleanest and safe [40], ease of manipulation [16] a portable, electricity-independent, almost zero carbon emission [2], inexhaustibility [41], abundant, a green, renewable and sustainable energy resource [9,42,43], utilization of less and free energy, elevated water evaporation rate straightforward operational procedures [44] and lack of environmental impact [45].

Recently, many solar vapor devices have been created with the primary purpose of capturing freshwater. However, there are many literature reviews available about photothermal conversion materials and the comprehensive architecture of such devices. Based to our knowledge there is no review discussed the role of textile materials in the ISSG. However, this review study thoroughly analyzes several textile materials, such as woven, nonwoven, and knitted textiles, as well as electrospinning membranes. It examines their specific functions and benefits in wastewater purification and desalination within the ISSG. Furthermore, this research emphasizes the challenges related to the progress of utilizing textile materials in Integrated Sustainable Sanitation and Greywater (ISSG) systems for wastewater purification. We also deliberated on potential opportunities and suggestions.

1.1. Interfacial Solar Steam Generation (ISSG):

Solar energy is a high-potential source of clean energy due to its abundance, renewable, inexhaustibility, and environmentally favorable nature, [37,46] it can be harnessed and transformed into various forms, including light, heat, and electricity [37]. However, it is widely recognized as a potential energy source in several applications [47], including but not limited to hydrogen production, power generation [48], photovoltaic, photocatalysis, desalination [49] and water treatment [50,51]. The ecological problems and high energy usage associated with conventional water purification techniques have spurred the development of alternative technologies [52], such as solar interfacial evaporation. These emerging technologies aim to address the limitations of conventional methods by utilizing renewable energy sources, improving energy efficiency, and minimizing environmental impacts [30]. Conventional methods of solar evaporation typically exhibit a relatively low photothermal conversion efficiency ranging from 30% to 45% [15,53]due to inadequate solar absorption and significant heat dissipation resulting from the positioning of the light absorber at the bottom of the water source. Consequently, the practical implementation of this approach could be improved [46].

ISSG can effectively harness solar energy in order to heat the liquid located at the interface between water and air, hence facilitating the formation of steam. However, photothermal materials

Preprints (www.preprints.org) | NOT PEER-REVIEWED | Posted: 28 December 2023 doi:10.20944/preprints202312.2214.v1

are capable of absorbing and converting solar radiation into heat energy [54]. These materials typically have high light absorption properties across a broad spectrum, including visible and near-infrared wavelengths. When exposed to sunlight, the photothermal materials absorb the photons and convert their energy into thermal energy [47]. However, in order to enhance the effectiveness of interfacial evaporation, inorganic and organic absorbers photothermal materials, such semiconductor nanomaterials [8,51,55], plasmonic nanoparticles [56], metallic nanoparticles [57], Mxene [58], carbon derivatives [50] such as carbon black [17,29,30,41,53], activated carbon [48], carbon nanotubes [37], carbon fibers [59] and grapheme oxide [22] have been suggested as potential mediums for converting sunlight into heat, most of these absorbers have been coupled with floating structures of ISSG devices. However, among these materials, carbon-based materials exhibit favorable photo-stability across a broad spectrum of wavelengths ranging from 200 to 2500 nm. Additionally, they possess exceptional chemical resistance, rendering them resistant to acidic, alkaline, and saline solutions. Furthermore, their flexible construction capabilities make them desirable for effective solar-driven evaporation applications [60]. Photothermal materials are strategically positioned on the water's surface, where they promptly generate heat at the interface between the air and water. This technique effectively prevents the bulk water from being heated, resulting in higher efficiency when compared to conventional thermal distillation methods [20].

Certain essential requirements and the overall principles and material and designing parameters must be met to optimize solar-vapor conversion performance of ISSG system are shown in **Figure 1(a, b)**. These principles encompass (i) The ability to effectively absorb solar light across a wide range of wavelengths, (ii) The localization of heat at the interface between air and water, (iii) A sufficient supply of water to sustain continuous evaporation and (v) The presence of suitable pores facilitates the avoidance of vapor [21,25]. Solar interfacial evaporation has the potential to contribute significantly to alleviating global freshwater scarcity, particularly in sunny and water-stressed regions. Ongoing research and development efforts aim to enhance the technology's efficiency, durability, and cost-effectiveness, making it a viable solution for sustainable freshwater production in the future.

Preprints (www.preprints.org) | NOT PEER-REVIEWED | Posted: 28 December 2023 doi:10.20944/preprints202312.2214.v1

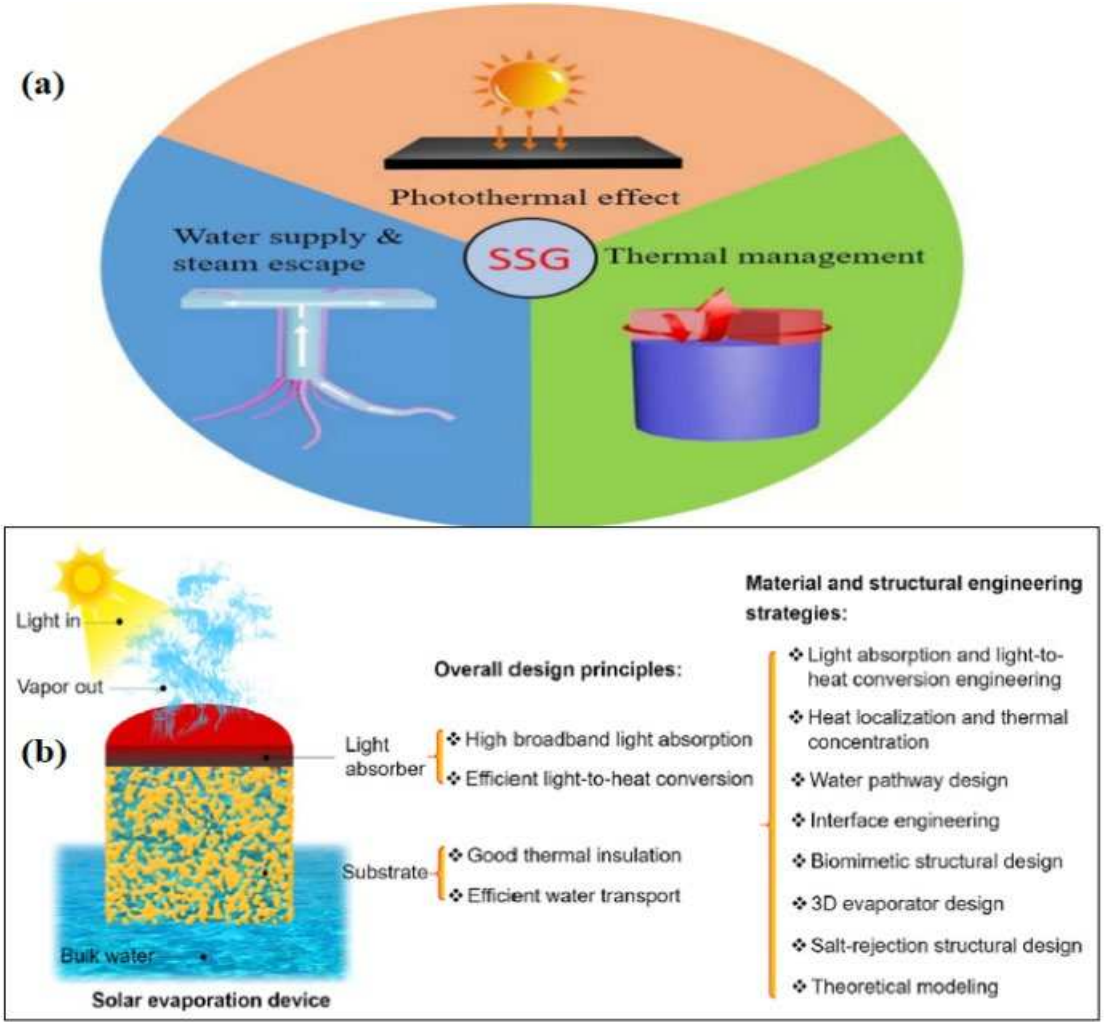

Figure 1. (a) Three main factors for ISSG design [61] copy right 2019 The Royal Society of Chemistry (b)The overall principles and material and designing parameters of SSG system [46] copy right 2018 Elsevier.

1.2. Fundamental principles for the design of ISSG devices:

1.2.1. The sunlight absorption:

Solar-driven evaporated water, regarded as a fundamental thermodynamic phenomenon, has been extensively employed in various applications in historical and contemporary contexts, encompassing both natural and industrial settings. The solar-powered evaporation system can be categorized into three classifications based on the positioning of the photothermal material within the fluid. The first system under consideration is a conventional bottom-heating-based evaporation method. The second system is a suspended evaporation system. Lastly, the third system is a solar steam generation system [15]. However, solar vapour generation, a process that utilizes solar thermal energy to induce water evaporation without the need for supplementary energy, presents a straightforward approach to address the challenges of water purification or desalination [53].

Solar steam systems can be categorized into three distinct heating ways, namely bottom heating, bulk heating, and interfacial heating, based on placing the photothermal substance **Figure 2 (a-c)**. The process of bottom heating involves the transformation of solar energy into thermal energy, which is then utilized to immobilize active components at the lower region of a water body. Using this approach causes the application of heat to a significant portion of the aqueous environment. The process involves evenly dispersing plasma nanoparticles, which serve as the photothermal material, across the water body to achieve bulk heating. Interfacial heating refers to placing a photothermal

Preprints (www.preprints.org) | NOT PEER-REVIEWED | Posted: 28 December 2023 doi:10.20944/preprints202312.2214.v1

substance at the interface between air and water, resulting in the concentration of light only on a narrow layer of water on the evaporation surface [62].

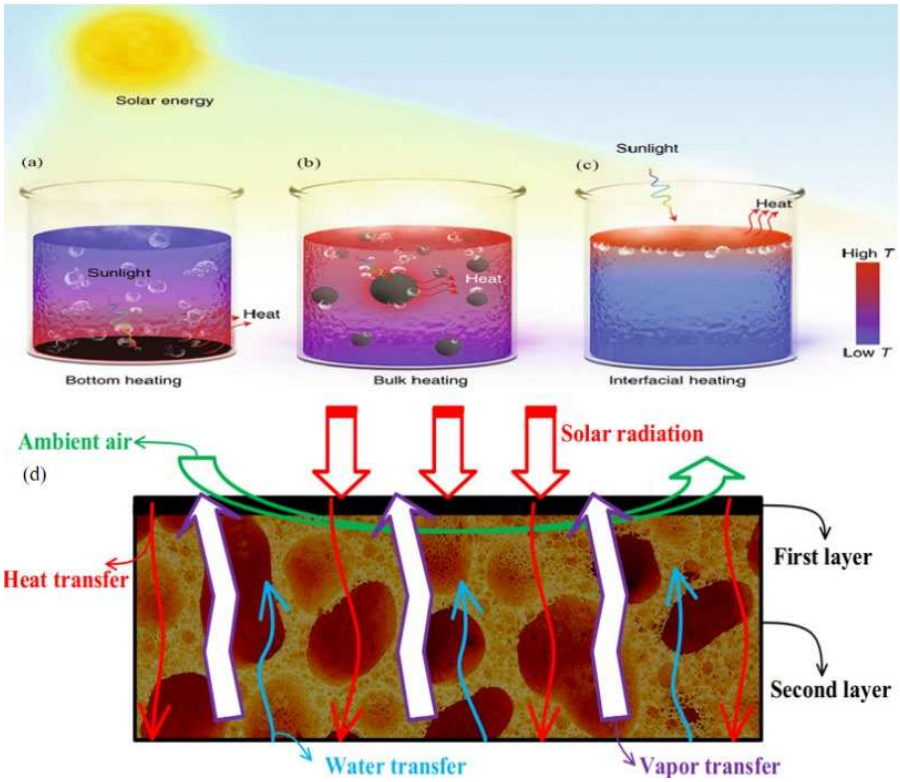

Figure 2. ISSG different method of solar heating (a) Bottom heating model(b) Bulk heating model (c) Interfacial heating model [62] copy right 2023 MDPI. (d) The process of the heat and mass transfer in the bottom layer [63] copy right 2018 Elsevier.

ISSG typically involves the use of photothermal materials that absorb sunlight and convert it into heat **Figure 2 (d)**. These materials can be incorporated into various configurations such as solar stills, solar evaporators, or solar collectors. When exposed to sunlight, the photothermal materials absorb the solar radiation and heat up, raising the temperature of the surrounding water. As the water reaches its boiling point, it evaporates, leaving behind impurities and contaminants. The vapor is then condensed and collected as clean water, separate from the contaminants [64]. The property of efficient absorption within the sun spectrum is essential when considering a material's suitability for solar heat localization. The solar spectrum encompasses wavelengths ranging from around 300 nm to 2500 nm. The selected material must possess high absorption efficiency within this specific range of wavelengths, resulting in minimal losses due to reflection and transmission [65]. However, in order to obtaining high solar vapor conversion rates is contingent upon two crucial factors: firstly, the maximization of solar energy absorption and heat conversion; and secondly, the reduction of heat loss while improving the distribution of energy for water evaporation [53].

1.2.2. The principles of ISSG design:

The term photothermal refers to the phenomenon in which the application of light stimulation results in the generation of thermal energy, either partially or entirely. The efficiency of photothermal evaporation is reduced below 100% due to the inevitable heat loss that occurs as a result of heat conduction and heat radiation during these procedures **Figure 3 (a)**. The capacity of a substance to effectively absorb and utilize light is a fundamental factor in the process of photothermal transformation. The two aspects of interest in this context are the extent of absorption across the solar spectrum and the magnitude of absorption at different wavelengths [66]. During a standard measurement technique **Figure 3 (b)**, the ISSG device is immersed in a container containing either

Preprints (www.preprints.org) | NOT PEER-REVIEWED | Posted: 28 December 2023 doi:10.20944/preprints202312.2214.v1

clean water or brine for desalination experiments. Additionally, a solar simulation device is positioned over the apparatus to emit simulated sunlight flux. It is recommended that the size of the light sources be significantly larger than the area of the sample. The level of illumination can be adjusted to any desired power level. However, it is strongly recommended to maintain an illumination level of 1 kW m² (1 sun) due to the dispersed nature of natural sunshine on the planet [67].

The solar-to-vapor conversion efficiency (η) was determined by evaluating the evaporation rate by utilizing the following equation: [17,52,64,65]

$$\eta = \frac{m \,.\, h\, lv}{p\, l} \qquad (1)$$

where m is the water evaporation rate (kg m^{-2} h^{-1}), h_{LV} is the total enthalpy of water–vapor phase conversion and ρ_L is the light power density (Wm^{-2}). While the evaporation rate can be calculated via the following formula: [13]

$$V = \frac{1}{A\,evap}\frac{dm}{dt} = \frac{m}{A\,proj} \qquad (2)$$

where:

v: Evaporation rate (mass of water evaporated per unit time), m: Mass change of water, A_evap: Evaporation surface of the system (area over which evaporation occurs), t: Illumination time (duration of exposure to solar radiation).

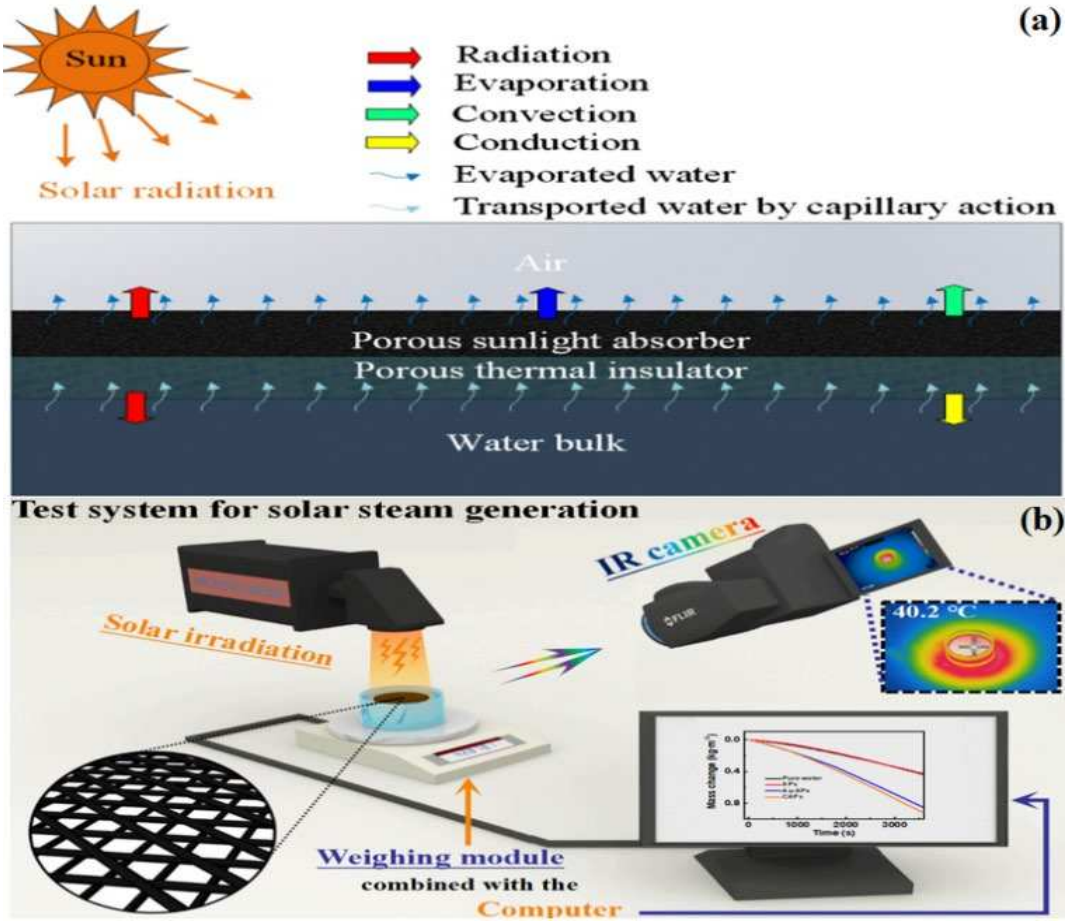

Figure 3. (a) The fundamental principles underlying the heat and mass transfer mechanisms within ISSG device [68] copy right 2018 Elsevier (b)The design to assess the SSG capability [57] copy right 2018 Frontiers Media S.A.

1.2.3. Water supply system in ISSG devices:

During the ISSG operation, water undergoes two primary processes. Firstly, water is absorbed from the reservoir into the photothermal interface. Secondly, water undergoes the process of heating

Preprints (www.preprints.org) | NOT PEER-REVIEWED | Posted: 28 December 2023 doi:10.20944/preprints202312.2214.v1

and subsequently transforms into steam, which is then dispersed into the surrounding air. Textile fabrics can facilitate the efficient absorption of water and steam transportation. To enhance evaporation efficiency, it is imperative to establish a state of equilibrium between the quantity of supplied water and the quantity of water that has evaporated. Significantly, in the water supply process, the presence of fibrous materials has the potential to decrease the energy needed for evaporation by lowering the enthalpy of evaporated water, hence resulting in an augmented rate of evaporation [54]. The effectiveness of solar steam generation systems is contingent upon several factors, including the ability to absorb sunlight, move water, facilitate water evaporation, and control temperature swings [69]. However, the design of water pathways plays a crucial role in the attainment of uninterrupted and effective water transportation. Moreover, the interfacial features of solar evaporation systems also hold significant importance. The primary characteristic of the contact that holds significant importance is its wettability. This feature is crucial in various aspects such as water conveyance, light absorption, gadget floating, and stability. The desirability of a hydrophilic interface, which encompasses the outermost layer, lies in its ability to facilitate water draining through capillary pumping. This design approach has been widely employed in developing absorber and water transport structures [46].

In textile materials, the spacing between fibers within the material is established through the arrangement of individual fibers that twist and intertwine with neighboring fibers, creating pathways for the transportation of water and steam. However, the dimensions of the porosity and the level of thickness of the fabric are critical variables in ascertaining water supply. In particular, pores of more excellent dimensions can facilitate enhanced water and steam transportation, while pores of more petite dimensions can augment the capillary forces [54]. Hydrophobic materials textile products such as cotton fabric has garnered significant attention recently due to its inherent hydrophobicity, remarkable gas permeation, exceptional mechanical characteristics, flexibility, and potential for scalability [70], with strong capillary effect [58]. However, the presence of a hydrophilic surface is of utmost importance in the process of high-efficiency solar-driven water vapor generation [71]. This is due to the fact that evaporation occurs primarily at the interface between air and liquid. As reported by Hao D. et al [72] they conducted a study on the effective generation of solar water vapor, facilitated by the utilization of water-absorbing polypyrrole coated cotton fabric that exhibits improved thermal localization **Figure 4**. The selection of cotton fabric in this context was based on its hydrophilic properties, inherent porosity structure, widespread availability, favorable mechanical stability, and cost-effectiveness. The result confirmed that PPy/cotton-foam structure demonstrates a solar thermal conversion efficiency of 82.4% when exposed to 1 kW/m^2 illumination with an elevated evaporation rate of 1.2 kg m^{-2}h^{-1}. The solar vapor generator demonstrated consistent reusability in a series of 30 cycle trials conducted under solar irradiation of 1 kWm^{-2}. The aforementioned findings suggest that the implemented interfacial water evaporation system plays a beneficial role in alleviating the problem of freshwater scarcity.

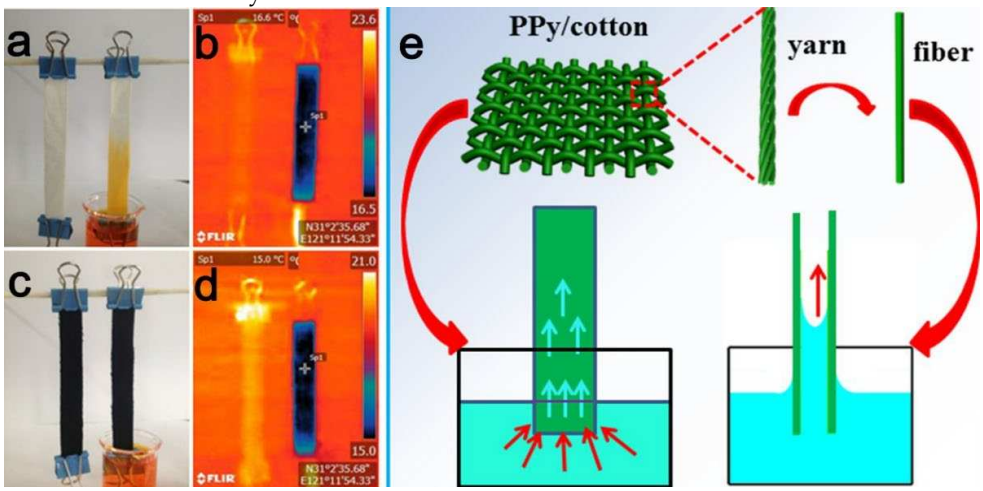

Figure 4. the optical images illustrating the vascular absorption of water of pristine cotton (a) PPy/cotton (c) IR photos demonstrate the temperature variations of pristine cotton (b) and PPy/cotton

Preprints (www.preprints.org) | NOT PEER-REVIEWED | Posted: 28 December 2023 doi:10.20944/preprints202312.2214.v1

(d) both before and after capillary absorption (e) the process of capillary water absorption in PPy/cotton fabric [72] copy right 2018 Elsevier.

2. The role of textile materials in ISSG systems:

Textile materials find extensive application in various sectors, including fashion, sportswear, home textiles, medical textiles, automotive textiles, and many more. The combination of their thinness, lightweight nature, flexibility, comfort, a high degree of flexibility. Additionally, they exhibits a porous structure that can be easily scaled up for industrial production [73]. Furthermore, they demonstrates excellent durability and the capacity to be programmed to achieve desired pore structures makes them highly suitable for a wide range of products and purposes [74]. Recent advancements in the field of water transmission through textiles materials of varying dimensions have provided novel approaches for the development of floating structures aimed at water evaporation. These include techniques such as utilizing hanging of (woven, non-woven, knitting) fabrics, composite [41] and electro-spun membranes [3]. However, this technique involves suspending or hanging fabric materials over a water surface. The fabric acts as a medium for water transmission and evaporation. As water molecules evaporate from the surface, they pass through the fabric, allowing continuous evaporation. The structure of the fabric provides a large surface area for evaporation, enhancing the efficiency of the process. However, the following unique features of the textile materials render them highly promising for solar interfacial evaporation: (i) Fabrics have a textured and rough surface, which enhances their light-absorption abilities. The roughness increases the surface area available for solar radiation absorption, allowing for efficient conversion of solar energy into heat. (ii)Textile materials typically have high porosity and a significant surface area. These characteristics provide an extensive evaporation area, allowing for a larger interface between the liquid and the surrounding air. Additionally, the porosity of textiles creates multiple pathways for the steam to escape, reducing the chances of re-condensation. (iii)Textile materials are known for their exceptional flexibility and robust mechanical strength. They can be easily manipulated and shaped into desired configurations, allowing for the creation of portable and scalable devices. (v)Fabrics are typically cost-effective and readily available materials. The affordability of textiles ensures that the technology can be more accessible and economically viable for widespread implementation, especially in areas with limited resources [54,75]. Moreover, Textile materials possess a wide range of raw ingredients, a diverse array of adaptable manufacturing methods, and a high degree of flexibility [54].

The absorbers employed in a solar interfacial evaporator have been fabricated utilizing a diverse range of substances, including foams, aerogels [11,32,52,69], hydrogels [76], films, membranes [2,77], biomaterials and textiles [58]. Within this assortment of materials, there exists a range of textile materials, including woven fabrics [45,75], knitted fabrics, nonwoven fabrics [71], composites materials [78] and other. However, textile materials possess the characteristic of having an adjustable texture and including microsized pores [71], enabling the effortless cleansing of soiled fabric. Moreover, these fabric exhibit commendable endurance, facilitating the effective elimination of impurities [79]. The characteristics mentioned above have piqued many researchers' curiosity in advancing adaptable and launderable photothermal textiles that possess micronized pathways and incorporate the encapsulation of photothermal nanoparticles.

2.1. Woven Fabrics:

Woven technology is usually applied to produce woven fabrics through the systematic interlacing of warp and weft threads, resulting in fabrics that exhibit favorable attributes such as high tensile strength, resilience to wear and tear, dimensional stability, and a dense structure [54]. Textile products possess a modifiable structure and contains micronized pores, enabling the effortless cleansing of filthy garments. Additionally, these fabrics exhibit commendable longevity, facilitating the effective elimination of impurities [79]. However, cotton has become known as the primary natural fiber utilized in the textile industry due to its inherent characteristics such as natural softness, significant hygroscopicity, exceptional wear comfort, and skin-friendly properties [80]. By employing

Preprints (www.preprints.org) | NOT PEER-REVIEWED | Posted: 28 December 2023 doi:10.20944/preprints202312.2214.v1

a practical textile weaving method, Zhang Q. et al [75] presented a ISSG device composed of a blend of carbon fiber and cotton yarn **Figure 5 (a, b)**. This device has remarkable capabilities in generating solar steam, owing to the carbon fiber's reliable and efficient light-absorbing properties, as well as the unique structure of the fabric. The manipulation of woven fabric design has the ability to control the levels of light absorption and amount of water within the cloth. Under 1 sun light, the modified fabric demonstrates a notable efficiency rate of 1.87 kg m^{-2} h^{-1} and evaporation efficiency of 83.7%. An all-encompassing and expansive apparatus, equipped with anti-salt clogging capabilities, may be readily achieved through the manipulation of warp thread count and weft thread width. The fabric that has been constructed exhibits considerable promise in the realm of obtaining cost-effective purification of seawater and other forms of wastewater. Consequently, it offers a novel avenue for the advancement of solar interfacial evaporators that are characterized by their high efficiency, scalability, and stability.

Using a conventional loom, Li Y. et al. [45] created a 3D hierarchical tree-shaped biomimetic flax fabric (TBFF) **Figure 5 (c)**. The design comprised a float layer, a basket weave layer, and a plain weave layer. The fabric exhibited vertical water transport properties along the uninterrupted warp strands. Subsequently, the TBFF that was acquired underwent a one-step manufacturing process to produce polydopamine-polypyrrole hybrid (PDA-PPy) nanofibers with more surface space and enhanced hydrophobicity. However, the fabricated design demonstrates an ordered structure of micro-capillary porosity within the fibers and macro-interlaced pore spaces across the warp and weft threads. This unique design enables the system to display spectrum light absorption, efficient water supply, a wide evaporation area, and easy steam escape. Hence, the interconnected water transport pathways established by TBFF-PDA-PPy demonstrated a notable evaporation rate of 1.37 kg m^{-2} h^{-1}, with a solar energy transformation performance of 87.4% when subjected to 1 sun irradiation. Due to its straight forward fabrication method, cost-effectiveness, and potential for scalability in manufacturing, the device has promise for facilitating widespread implementation in water filtration and saltwater desalination.

Additionally, a novel approach to fabric draping that involves the separation of the evaporation interface from the bulk water is designed by Gao C. et al [17]. However, the drape fabric is a coated by a mixture of carbon black (CB) and crosslinked sodium alginate (SA) onto ramie fabric (CSRF). The CSRF exhibited an evaporation rate of 1.81 kg m^{-2} h^{-1} and an efficiency of 96.6% when subjected to 1sun. Furthermore, manipulating yarn fineness in the fabric create an adjustable water supply system, thereby optimizing energy distribution. This study presents a novel approach to designing and optimizing solar evaporation systems, showcasing significant promise for practical implementation.

Preprints (www.preprints.org) | NOT PEER-REVIEWED | Posted: 28 December 2023 doi:10.20944/preprints202312.2214.v1

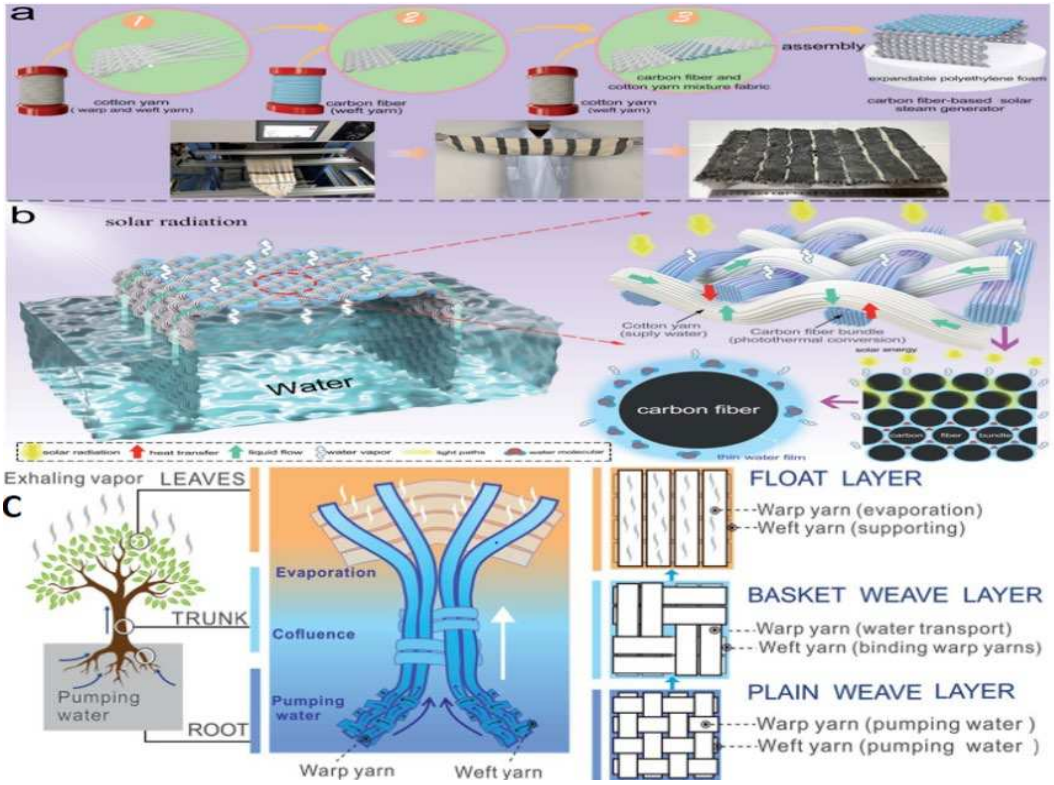

Figure 5. (a) The manufacturing of the CCMF based ISSG including the design of CCMFs by a textile weaving technique. (b) The operation concepts of CCMF based ISSG [75] Copy right 2020 The Royal Society of Chemistry (c) Schematic illustration of the tree shape and the representing biomimic design of the TBFF [45] copy right 2021, The Royal Society of Chemistry.

Composite fabric combines two or more fibers or materials to create a single fabric with improved qualities. The blended fabric's combination of materials enables the effective utilization of each component's capabilities, leading to a fabric that exhibits enhanced performance qualities. Wang Y. et al [58] constructed a novel composite material of MXene, carbon nanotubes, and cotton fabric using a layer-by-layer assembly technique **Figure 6 (a)**. This fabrication aimed to develop a material capable of ISSG for purifying textile effluent. The device significantly enhanced optical absorption, light-to-thermal conversion, and water transport capabilities due to its significant interfacial contacts. Under1solar illumination, the evaporation rate for pure water is 1.35 kg $m^{-2}h^{-1}$, while for textile wastewater, it exceeds 1.16 kg $m^{-2}h^{-1}$ with an evaporation efficiency of 88.2%. These values are higher than those observed in the prior research for fabric-based composites. Reducing the amount of organic-inorganic pollutants in condensed fresh water is a crucial aspect that is often overlooked but holds significant importance in practical applications. In addition, the reusability test and outdoor experiment were conducted to showcase the practical application of the photothermal features. Furthermore, the findings of this study indicate that the composite material possesses superior performance and durability, as well as a straightforward fabrication procedure. These characteristics render it a promising option for wastewater purification using solar evaporation. A three-dimensional (3D) ISSG device in the shape of a cone is developed by He M. et al [81]. However, the device is consisted cotton fabric coated with vertical polypyrrole nanowires (VPPyNWs) **Figure 6 (b).** However, the polypyrrole (PPy) microstructure enhances solar energy absorption by facilitating simultaneous reflections between the vertically aligned PPy nanowires (VPPyNWs). The overall architecture of the 3D evaporator is characterized by an increased surface area, which promotes efficient energy harvesting, a comprehensive pathway for water supply, and an open structure that facilitates vapor diffusion. The 3D VPPyNWs-fabric-based SSG, obtained to demonstrate its feasibility, exhibits a rapid rate of water evaporation 2.32 kg m^{-2} h^{-1}. Additionally, it showcases a high solar absorption performance of 97% and a solar-to-vapor conversion efficiency of 98.56% when subjected to an energy density of 1 kW m^{-2}. Furthermore, the SSG can be effectively utilized in diverse

Preprints (www.preprints.org) | NOT PEER-REVIEWED | Posted: 28 December 2023 doi:10.20944/preprints202312.2214.v1

water conditions, such as seawater, dye wastewater, and acidic and alkaline wastewater. The effective use of solar energy can be significantly enhanced by implementing a high-performance evaporator incorporating a 3D macro- and structural design. This innovative approach presents a promising opportunity for improved solar energy utilization.

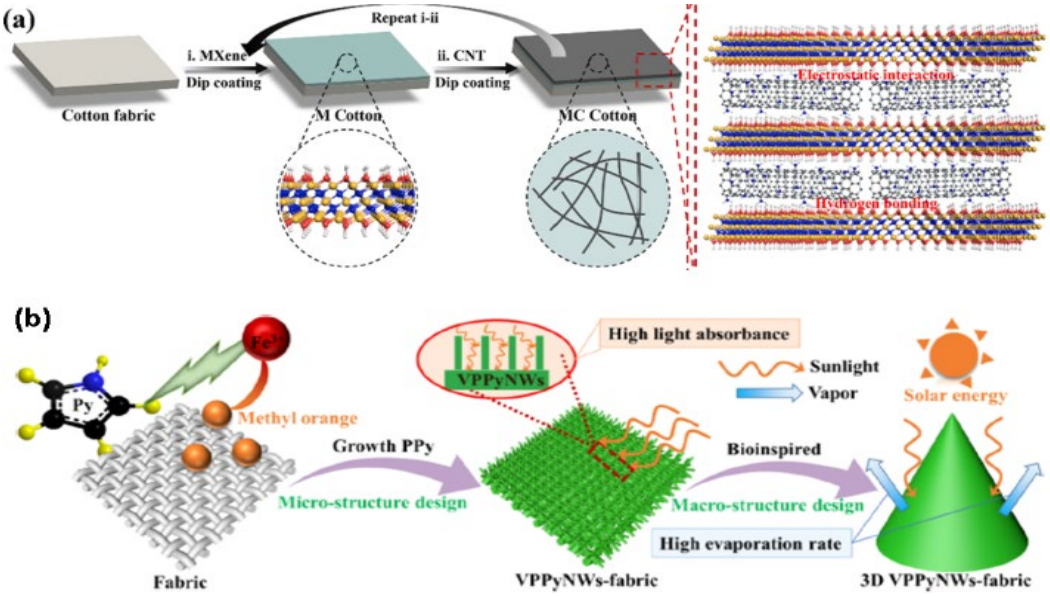

Figure 6. (a) Diagram of L-b-L fabrication of MXene nanosheets and CNTs on cotton fabric [58] copy right 2020 Elsevier. (b) Fabrication of 3D VPPyNWs-Fabric [81] copy right 2021 American Chemical Society.

A cost-effective and reusable SSG device fabric based is successfully fabricated by Kou H. et al [34] via applying carbon nanotube (CNT) based ink to conventional cotton fabrics. However, the cotton fabrics colored with CNT, demonstrate significant optical absorption within the wavelength range of 250–2500 nm, resulting in a total solar absorption efficiency of 95.7%. However, with utilizing polystyrene (PS) foam as the thermal insulator, the cotton-carbon nanotube fabrics with insulating properties demonstrate a notable evaporation rate of saltwater 1.59 Kgm^{-2} h^{-1}. Additionally, the apparatus possesses the capability to undergo cleaning and recycling processes through the elimination of the salts that are generated. Following evaporation, the liquid is effectively removed using a straightforward hand-washing procedure. This study demonstrated the feasibility of achieving cost-effective, highly efficient, and large-scale seawater desalination using solar irradiation.

Hydrophilic fabrics are designed to quickly wick away moisture from the skin, spreading it across a larger surface area to enhance evaporation and promote a dry and comfortable feeling. However, a highly hydrophilic, linear, and durable copper-based metal-organic framework (Cu-MOF) is designed by Wang J. et al [82] an absorber coating is securely attached to the surface of a commercially available textile material through the utilization of a sputtered copper film as a bonding layer **Figure 7 (a)**. However, the Cu-MOF photothermal fabric based demonstrated effective prevention of salt formation on its upper surface, even when exposed to a salinity of 9.5 wt% for over 12 hours during evaporation. This can be attributed to the CMPT's exceptional capillary effect and strong water-pumping performance. The CMPT, characterized by its exceptional light absorbance (95.9%) resulting from the distinctive hierarchical structure of Cu-MOF that enhances light trapping, and its excellent air permeability, demonstrated a significant evaporation rate of 1.52 kg/m^{-2} h^{-1} under 1 solar irradiation. The CMPT has a remarkable structural design, resulting in a high degree of adaptability, exceptional mechanical strength, and superb chemical stability even in demanding conditions. The study introduces an easy and uncomplicated method for surface immobilization of MOF coatings on textile fibers. This method has potential practical applications in the development

Preprints (www.preprints.org) | NOT PEER-REVIEWED | Posted: 28 December 2023 doi:10.20944/preprints202312.2214.v1

of portable solar steam generators. In another study done by Song L. et al [31] an innovative method is used for developing an effective ISSG using linen fabric with candle soot **Figure 7 (b)** . The system combines broadband light absorption, super-hydrophilicity, and an exceptional transition layer of water between a solar evaporator and an insulating material. This design aims to optimize the temperature control and water supply synergistically. By integrating improved energy management techniques and ensuring an ample water supply, the ISSG that has been developed demonstrates a commendable evaporation rate of 1.44 kg $m^{-2}h^{-1}$ and a high efficiency of conversion. The solar irradiation of 1 sun resulted in a solar-to-thermal conversion efficiency above 90% in salt water with a concentration of 20 wt %. The study has the potential to introduce a novel and straightforward approach to the water purification field.

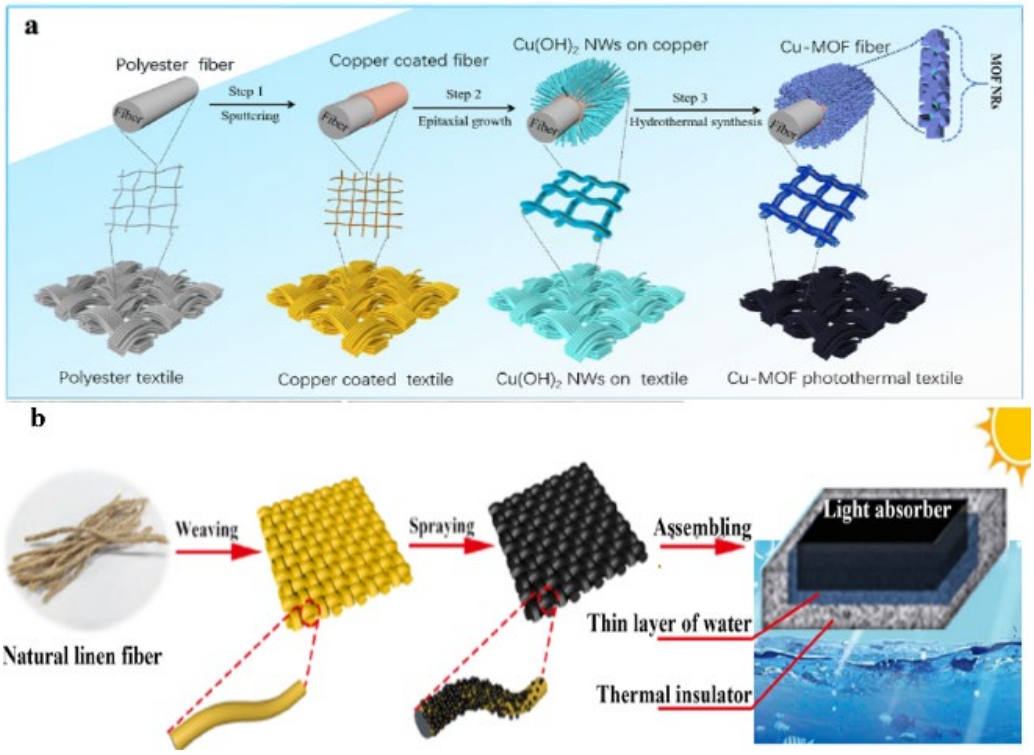

Figure 7. (a) Schematic illustration of the synthetic process for CMPT [82] copy right 2021 Elsevier (b) the natural linen fiber, the original linen fabric (LF), the LF covered with candle soot (LFS), and the integrated LFSTM composed of LFS and a thermal management section (polystyrene). SEM images of original linen fiber [31] copy right 2020 American Chemical Society.

In a study done by Peng H. et al [83], a new device of fluidic evaporator is developed, which exhibits asymmetry and enables edge-preferential crystallization. The device facilitates gravity-assisted salt collection and drenching-induced electrokinetic power generation, it is fabricated by spreading TA-MoS_2 nanosheets unevenly on a UIO-66-NH_2-modified PAN fabric as shown in **Figure 8 (a)**. The system utilized self-manipulated saline water transport to derive benefits, it effectively isolates the crystallized salts from the evaporation surface, facilitating uninterrupted vapor generation and salt extraction for 60 hours in sun desalination processes involving saline solutions with a concentration of 7.5 wt%. This wet fabric evaporator achieves a sustained voltage generation of 0.568 V solely through saline-drenching by utilizing the established gradient electric double layers in asymmetric nanochannels. In addition, the evaporator exhibits a high capacity for effectively removing organic pollutants, with minimal impact on both the water evaporation and power generation rate, even after 60 hours of continuous operation and 30 cleaning instances with an evaporation rate of 1.36 kg $m^{-2}h^{-1}$ and a high efficiency of conversion about 89.2%. This study showcases a scalable multifunctional asymmetric solar evaporator that enables continuous seawater desalination, facilitating salt harvesting and electricity production. Furthermore, it contributes to the

Preprints (www.preprints.org) | NOT PEER-REVIEWED | Posted: 28 December 2023 doi:10.20944/preprints202312.2214.v1

progress of adaptable and environmentally friendly applications in useful seawater desalination, specifically to recover resources, power generation, and storage.

The fabrication of self-floating Janus cotton fabric coated with a polyester woven fabric, which can reject salt, has been effectively designed by Gao S. et al [84] for ISSG system **Figure 8 (b)**. The device with controlled soot deposition exhibit solar absorption properties and the necessary superhydrophobicity to enable flotation on water, the Janus evaporator demonstrates a sustained evaporation rate of 1.37 kW m^{-2} h^{-1} and achieves an efficiency of 86.3% when subjected to 1 sun irradiation. Furthermore, it exhibits satisfactory performance under conditions of minimal intensity and tilted radiation. The foldable Janus absorber, which boasts a cost of less than $1 per square meter, exhibits great potential as a portable solar vapor generator.

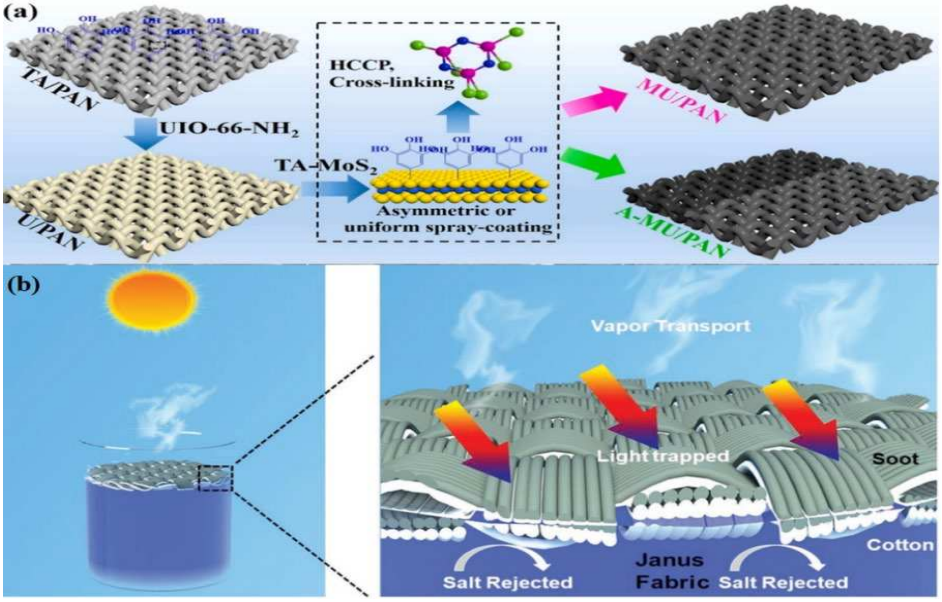

Figure 8. (a) Fabrication process of MU/PAN fabric [83] copy right 2021 Elsevier (b) design of the soot-deposited Janus fabric floating on the water surface [84] copy right 2019 WILEY.

Drawing inspiration from the Janus water absorption observed in lotus leaves, Qin Z. et al [85] developed a bio-inspired combination consisting of cotton fabric supplemented with carbonized carrot powder (CC powder) and coated with Nafion on one side (cotton cloth-NCC). This system has been designed to achieve enhanced efficiency in SSG. The utilization of CC powder in cotton fabric-NCC serves as a means to enhance light absorption, hence achieving a heightened level of light absorption. Simultaneously, the hydrophilic nature of the cotton cloth facilitates effective water transport. In the interim, applying Nafion coating creates a Janus architecture with hydrophobic and hydrophilic properties. This structure serves the dual purpose of regulating water supply and inhibiting salt deposition, even when exposed to high-concentration salt solutions. The cotton cloth-NCC material has undergone further processing to form a waved structure, resulting in w-cotton cloth-NCC. This modification aims to enhance the surface area available for water evaporation and obtain a high light absorption level, specifically reaching 95%. When exposed to solar irradiation, the utilization of w-cotton cloth-NCC results in a water steam generation rate of 1.88 kg m^{-2} h^{-1} and a saltwater evaporation rate of 1.52 kg m^{-2} h^{-1}. In addition, the w-cotton cloth-NCC has a notable efficacy in purifying sewage. It effectively eliminates Escherichia coli, achieving 100% removal while demonstrating a high removal rate of 98.3% for Rhodamine B. The methodology proposes a straightforward technique for fabricating a hydrophobic-hydrophilic Janus solar steam evaporator that is characterized by excellent efficiency, inexpensiveness, environmentally friendly operation, and long-term stability. This innovative design exhibits significant potential for use in various fields, including environmental purification and photothermal conversion. Additionally, a novel ISSG device was developed by Wang K. et al [86] by using thermally-treated pre-oxidized polyacrylonitrile fibre fabric combined with carbonized polyaniline nanowires (ECFC/CPANW) as shown in **Figure 9 (a)**. However, the system exhibits several advantageous characteristics, including low thermal

Preprints (www.preprints.org) | NOT PEER-REVIEWED | Posted: 28 December 2023 doi:10.20944/preprints202312.2214.v1

conductivity, efficient absorption of solar radiation across a wide range of wavelengths, favorable hydrophilic properties, and excellent water transport capabilities. The results showed a remarkable vaporization efficiency of up to 93.7% with an evaporation rate of 1.43 kg m^{-2} h^{-1} when subjected to 1 sun irradiation. Hence, using cost-effective, stable, and environmentally friendly photo-thermal conversion materials holds significant potential for real-world use in water purification processes.

A novel composite membrane of MXene, carbon nanotubes, and cotton fabric is fabricated by Wang Y. et al [58] by using a layer-by-layer construction technique as ISSG device **Figure 9 (b)**. Due to its robust surface contacts, the hybrid fabric significantly enhanced optical absorption, light-to-thermal conversion, and water transport capabilities. The evaporation rate for water is found to be 1.35 kg $m^{-2}h^{-1}$, while for textile wastewater, it exceeds 1.16 kg $m^{-2}h^{-1}$ under 1 solar illumination. In addition, the reusability test and outdoor experiment were conducted to showcase the photothermal characteristics of the material when implemented in real-world scenarios. The results indicate that the combined material possesses favorable characteristics such as excellent performance and durability, as well as a straightforward fabrication technique. Thus, it holds promise as a viable option for wastewater purification by solar-evaporation methods.

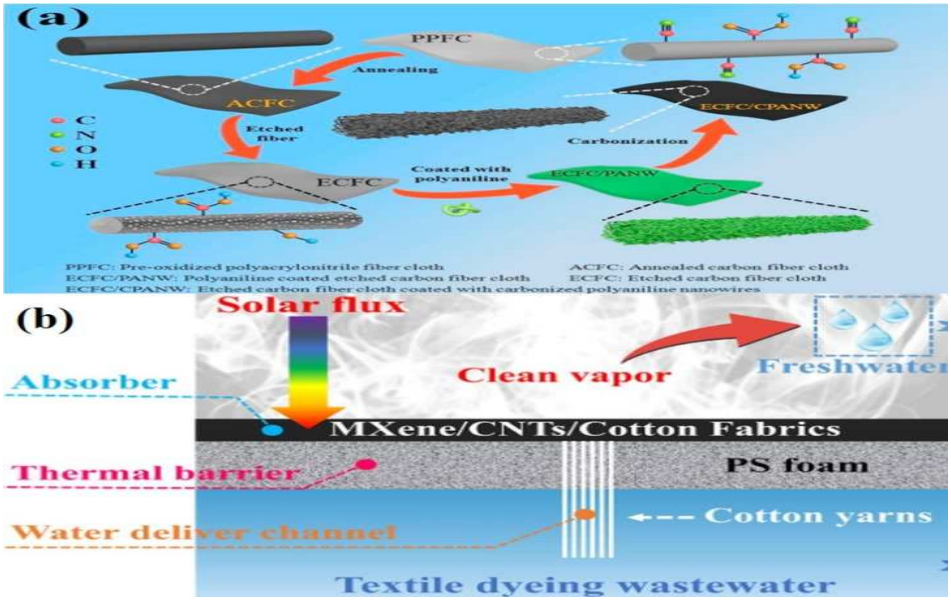

Figure 9. (a) The preparation of ECFC/ CPANW SSG device [86] copy right 2019 Elsevier (b) MXene/CNTs/Cotton fabric ISSG device [58] copy right 2020 Elsevier.

Peng H. et al [69] presented a novel approach to purify seawater and power production by developing a one-way asymmetrical nanofluidic photothermal evaporator. The design of this evaporator is inspired by the water and solute transportation in plants, specifically through the transpiration process. The fabrication process involves the in-proportion deposition of photothermal MXene nanosheets on a hydrophilic cotton fabric. However, the cotton fabric pump facilitates the linear transportation of saline solution, allowing for self-operating salt rejection and stable steam generation in the evaporator. Additionally, forming an asymmetric double electrode layer within MXene nanochannels under the drenching state enables continuous electric power generation. The solar-induced evaporation rate and voltage generation achieve a value of 1.38 kg $m^{-2}h^{-1}$ with an efficiency of 83.1% and 363 mV, respectively, when exposed to 1 sun irradiation. Significantly, the aforementioned nanofluidic system exhibits minimal degradation in function following 30 hours of usage and undergoing 15 washing cycles. This observation underscores its exceptional stability and capacity for repeated use. The straightforward design of the asymmetric nanofluidic photothermal system presents potential opportunities to expand sustainable freshwater and electric power generation.

Carbon fibers derived from two types of animal silks, namely Bombyx mori (B. mori) silk and Antheraea pernyi (A. pernyi) silk, are fabricated by Qi P. et al [87] by using a single-step heating

Preprints (www.preprints.org) | NOT PEER-REVIEWED | Posted: 28 December 2023 doi:10.20944/preprints202312.2214.v1

process on a massive scale without the need for any additives or activation procedures. The carbon fibres and yarns possess both electrical conductivity and mechanical strength. To enhance the utilization of carbonized silks, we proceeded to interlace them with cotton yarns, resulting in the production of composite fabrics featuring diverse patterns **Figure 10 (a-e)**. The results verified the benefits associated with using hybrid fabrics, including enhanced light absorption, increased surface area, and hierarchical liquid transfer routes. These advantageous characteristics make these fabrics suitable for applications such as SSG for desalination and sewage treatment. Furthermore, it was observed that these conductive carbon fibers can be organized into fluidic nano-generators, enabling the generation of electrical energy by the movement of water.

Conventional photo-thermal materials primarily address concerns related to energy efficiency and multipurpose use. However, the absence of adjustable, affordable, adaptable, and washable characteristics significantly hampers their transition from laboratory settings to industrial applications. The achievement of enhanced energy efficiency is of great importance because of the limited utilization of spatial volume in traditional 2D evaporators. Consequently, there is a strong need for the advancement of customizable and programmable 3D designs. However, Xiao P. et al [88] fabricated a functional photo-thermal fabric that draws inspiration from conventional sewing techniques. The substance exhibits exceptional scalability, washability, and affordability. It enables the creation of tunable and programmable 2D/3D structures, facilitating efficient water extraction from liquid and solid mediums in both in-plane and out-of-plane directions. An in situ adjustable oxy polymerization approach was used to fabricate cotton fabric modified with polypyrrole (PPy) due to the favorable photo-thermal properties, stability, and effective contacts exhibited by PPy with fibrous cotton **Figure 10 (f)**. The device demonstrates a straightforward and robust method for synthesizing a large-area PPy-modified cotton (PMC) fabric. Moreover, the textiles possess commendable attributes such as sewability and editability, enabling the customizable incorporation of these functional PMC building blocks into 3D system to achieve highly effective out-of-plane solar vaporization. The 3D design can effectively integrate photo-thermal textiles into various surroundings, enabling efficient purified water extraction, even from a sandy substrate.

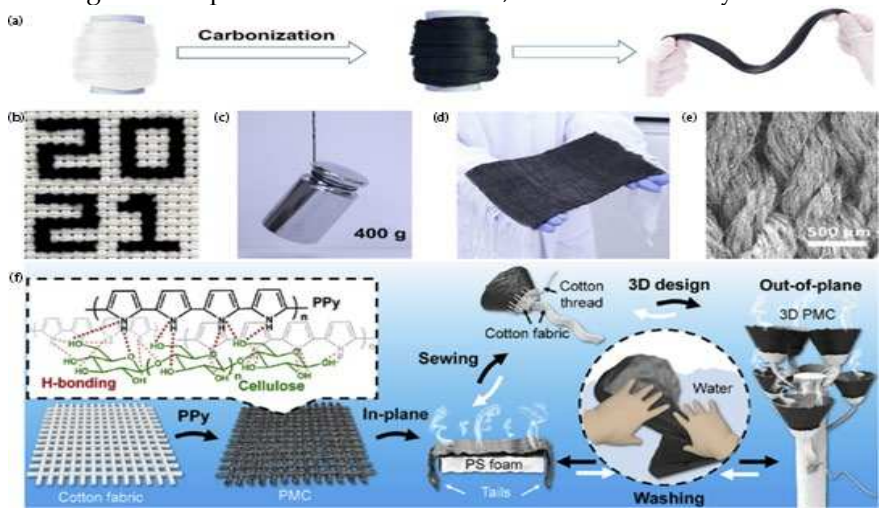

Figure 10. (a) photos of Bombyx mori (B. mori) silks before and after the carbonization; (b) "2021" is knitted by carbonized B. mori silks (CBSs); (c) A load of 400 g is lifted by CBSs (0.1 g); (d) A fabric is made of CBSs and cotton yarns; (e) The SEM image of a composite fabric; [87] copy right 2021 Sage. (f) Fabrication of functionalized cotton fabric as 2D/3D SSG [88] copy right 2019 Elsevier.

The fabrication of Janus ink/urushiol-modified cotton fabric was effectively designed by Bai W. et al [89] **Figure 11 (a, b),** resulting in the development of a fabric with distinct hydrophilic and hydrophobic properties. The Janus fabric exhibited exceptional characteristics in terms of water transportation, mechanical strength, thermal conductivity, and photothermal conversion efficiency. When subjected to simulated solar radiation, the temperature of the Janus cloth rose to 85 ◦C for 2 minutes. Furthermore, apparatus exhibited a notable conversion performance of 94.3% alongside a

Preprints (www.preprints.org) | NOT PEER-REVIEWED | Posted: 28 December 2023 doi:10.20944/preprints202312.2214.v1

remarkable evaporation rate of 1.64 kg m^{-2} h^{-1} with an adequate resistance to UV light and pH levels and a high capacity for rejecting salt in concentrated salt solutions. The system has shown significant efficacy in the purification of wastewater that contains heavy metals and organic dyes. A fabric that possesses many functions, including integrated ISSG and personal thermal control, offers a sustainable solution for addressing challenges related to water shortages and cold stress is designed by Du H. et al [90] by combination of graphene oxide photothermal absorber and low-cost hydrophilic Tencel fiber as water supplier **Figure 11 (c).** The regulation of photothermal conversion, water supply, and moisture diffusion capabilities can be achieved through the modification of loading, spinning, and twisting parameters. The fabrics that have been combined with whole-yarn-section photothermal capability demonstrate a noteworthy average evaporation efficiency of 90.4% and an impressive evaporation rate of 1.33. The exceptional cost-effectiveness of 222 g h^{-1} $\$^{-1}$ and the durability of 20 washing cycles and 15 operation cycles contribute to the great practicality of this device. In general, the GOT fabric offers a tailored solution for individuals engaging in outdoor activities, requiring garments that offer breathability and insulation, as well as portable devices for accessing clean water.

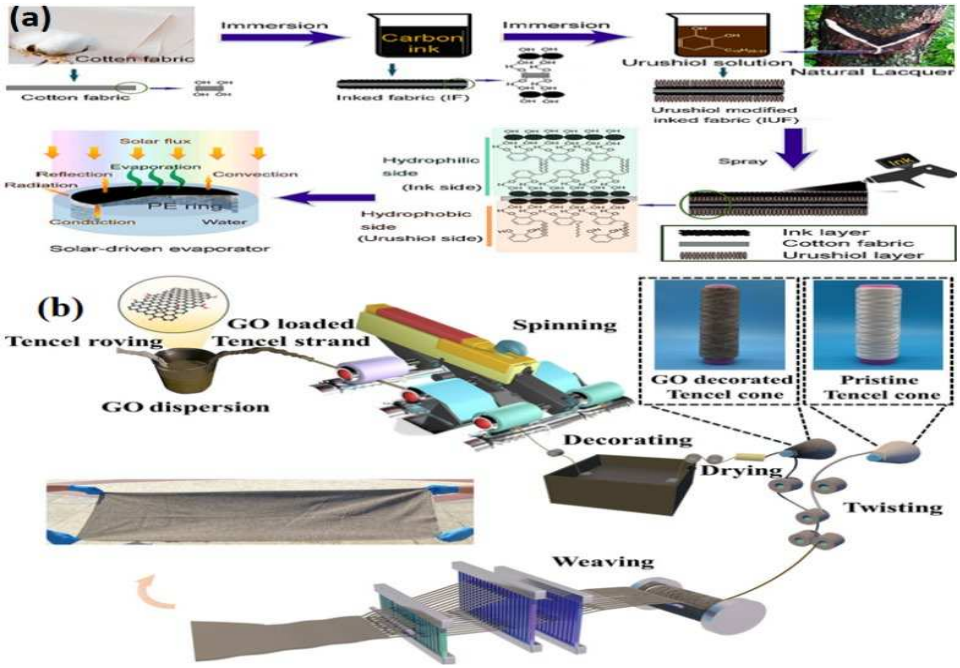

Figure 11. (a) fabrication of the Janus ink/urushiol fabric (b) energy balance of the SSG device [89] copy right 2023 Elsevier (c) the fabrication process of GOT fabric [90] copy right 2023 Springer Nature B.V.

A novel approach to boost freshwater production by integrating Janus fabric with thorough thermal control in a reversed ISSG is conducted by Gao C. et al [91]. However, an inexpensive Janus fabric, which incorporates recycled cotton fabric, is manufactured by applying a layer of carbon black@silicone on the top side using a straightforward and flexible pre-wet coating technique **Figure 12**. The Janus fabric possesses effective sealing capabilities that contribute significantly to the prevention of upward vapor formation, hence minimizing optical loss. Consequently, these characteristics of the Janus fabric contribute to the enhanced collection of freshwater in the distillation process. The Janus fabric-based interfacial solar distiller demonstrates a high level of sunlight absorbance, measuring at 98.0% and remarkable performance, with a water production of 1.17 kg $m^{-2}h^{-1}$ and an efficiency of 78% when exposed to one sun (1 kW m^{-2}) illumination. The study introduces an innovative design for a high-performance interfacial solar distillation system, which has the capability to be implemented on a large scale and at an affordable rate for industrial production purposes.

Preprints (www.preprints.org) | NOT PEER-REVIEWED | Posted: 28 December 2023 doi:10.20944/preprints202312.2214.v1

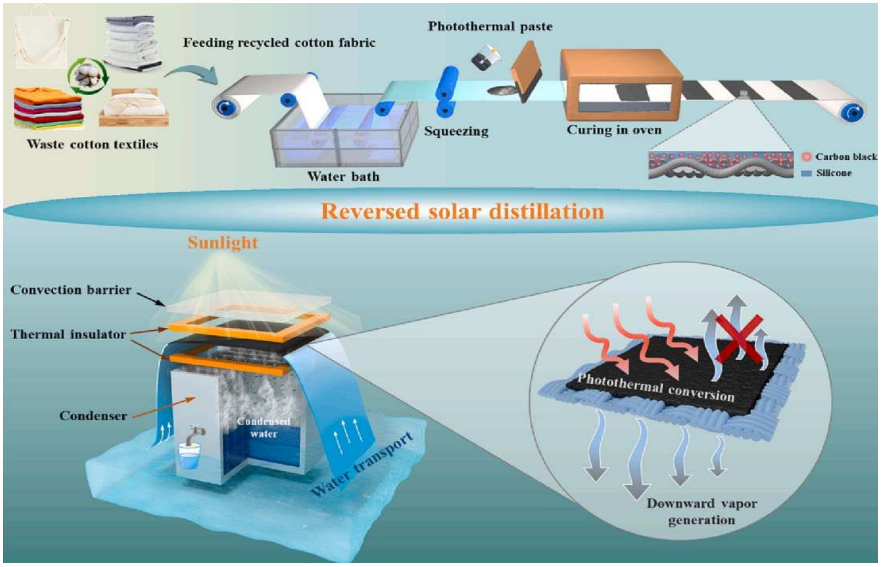

Figure 12. the process of the Janus fabric evaporator with coating process and the procedure of the Janus fabric based ISSG [91] copy right 2023 Elsevier.

2.2. Non-Woven fabrics:

Nonwoven fabrics are produced by aligning or haphazardly arranging staple fibers or filaments to create a fibrous network, which is subsequently strengthened through mechanical, thermal, or chemical processes, they has emerged as a promising and economically viable alternative for ISSG. This can be attributed to its numerous benefits, including the availability of copious raw materials, a straightforward manufacturing method, and the potential for excellent efficiency [54].

Sun S. et al [30] fabricated a carbon black (CB)-polydopamine composite non-woven fabric **Figure 13 (a).** This method sought a cost-effective and scalable PDA/CB@PP composite. In situ PDA polymerization and CB dip-coating were used to make the fabric. A hierarchical framework on the fiber's outermost layer and CB and PDA synergy produced high light absorbance (>95%), superhydrophilicity, and energy conversion efficiency. The experimental one-way fluidic PDA/CB@PP photothermal-based solar steam evaporator had a 1.68 kg $m^{-2}h^{-1}$ evaporation rate and 91.5% solar steam efficiency. PDA/CB@PP cloth purifies waters well despite salt. The hydrophilic porous fabric retains water channels and ensures a steady water supply. Additionally, the PDA/CB@PP fabric effectively treats heavy metal and chemical dye-polluted wastewater.

A solar evaporator that remains in a perpetual state of flotation is constructed by Zhu Y. et al [37] through the application of multiwall carbon nanotubes onto a bicomponent nonwoven material consisting of polypropylene/polyethylene core-sheath fibers **Figure 13 (b).** The all-fiber structure exhibits a high degree of porosity and ultra-lightness, accompanied by a substantial specific area. The design incorporates features such as enhanced water evaporation efficiency and interconnected passages to facilitate the effective escape of vapor. Additionally, the material should possess a low thermal conductivity in order to minimize heat dissipation. The water transport characteristics of the nonwoven material facilitate its ability to generate a pumping action autonomously. The relationship between water supply and loss has the potential to expedite the rate of water evaporation of 1.44 kg $m^{-2}h^{-1}$ with evaporation efficiency of 89.7% under 1 sun. The fabrication process involves the utilization of inexpensive resources and the implementation of industrialized techniques, resulting in the production of the final product.

The phenomenon of changeable texture and porous clothing being susceptible to pollution is widely acknowledged. However, it is commonly observed that such clothing may be effectively cleansed to eliminate any contaminants, while maintaining their original color and shape without any discernible alterations. However, Zhu B. et al [79] designed a washable, stretchable carbon-nanotube-embedded polyacrylonitrile nonwovens fabric using electrospinning technology. The wet fabric has a photo absorption efficiency of 90.8% and high photoabsorption in the 350-2500 nm region.

Preprints (www.preprints.org) | NOT PEER-REVIEWED | Posted: 28 December 2023 doi:10.20944/preprints202312.2214.v1

The cloth coated on polystyrene foam had shown a high seawater evaporation rate of 1.44 kg m^{-2} h^{-1} under simulated sunlight (1.0 kW m^{-2}). Simulations of high saltwater concentrations reveal solid salt deposition on fabric surfaces, leading to a significant decline in evaporation rate. The washing technique has minimal impact on fabric shape, photoabsorption, and evaporation, indicating longevity. The use of washable fabrics and parallel PS foams allows for the construction of large-scale outdoor evaporation devices, enabling successful desalination of seawater under natural sunlight.

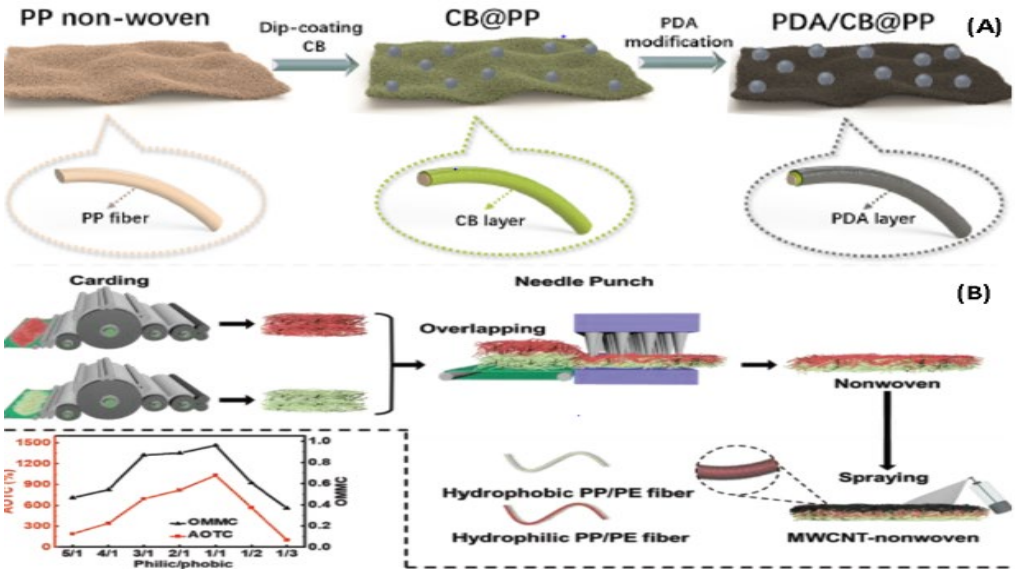

Figure 13. (a) Diagram of fabrication of the PDA/CB@PP samples [30] copy right 2021 Elsevier (b) The fabrication process of MWCNT-nonwoven with unidirectional water-transfer properties with hydrophilic/hydrophobic fibers [37] copy right 2021 Wiley.

A nonwoven photothermal cloth with exceptional stability, flexibility, and washability is fabricated by Jin Y. et al [41] via the process of electrospinning technology. The aim is to enhance the efficiency and longevity of solar steam evaporation. The fabric comprises polymeric nanofibers serving as the matrix, with inorganic carbon black nanoparticles embedded inside the matrix to function as the light-absorbing component. The photothermal fabric, which has been enhanced with an optimum carbon loading, exhibits a highly desirable characteristic of being black underwater. This fabric can absorb 94% of the sun spectrum, resulting in an impressive solar energy use efficiency of 83% within the process of pure water evaporation. Due to its unique composition and geometry, the fabric exhibits a characteristic resistance to photothermal component loss. It demonstrates exceptional flexibility and mechanical strength, as well as chemical stability in a wide range of challenging environments, including strong acids, alkaline substances, organic solvents, and saline water. The textile material can undergo hand-washing for over 100 cycles without experiencing performance degradation with evaporation rate 1.24 kg m^{-2} h^{-1} and evaporation efficiency 83%. This characteristic presents a promising approach for effectively removing fouling agents in real-world applications such as solar steam generation and distillation operations. In a previous study done by Fang Q. et al [71] a novel ISSG device with an exhibited exceptional light-thermal properties is designed by using activated carbon fiber fabric (ACFC) with tiny architectural structures **Figure 14 (a, b)**. However, Under optimal conditions, using cotton fiber nonwoven fabrics (CFNF) in a water supply system can significantly increase the evaporation rate, reaching 1.59 kg m^{-2} h^{-1}. Additionally, this system exhibits an impressive conversion performance of 93.3% when exposed to 1 Sun. The significance of achieving optimal alignment between water supply and vapor evaporation is underscored in maximizing heat utilization and enhancing the efficiency of solar desalination processes. Furthermore, the additional water supply pathway facilitated by CFNF effectively mitigates salt fouling by regular removal of salt deposits, ensuring the long-lasting performance of the self-cleaning solar steam generating system. Therefore, the ACFC+CFNF arrangement

Preprints (www.preprints.org) | NOT PEER-REVIEWED | Posted: 28 December 2023 doi:10.20944/preprints202312.2214.v1

demonstrates significant potential for utilization in permanent and extremely effective solar desalination.

The continual problem lies in achieving a balance between the expense and freshwater output. In order to address these issues, discrete waste carbon fibers are organized into a yarn that can be stretched and compressed by Wang J. et al [73]. This yarn is then processed for use in a fabric evaporator, which enables the creation of solar steam. This is achieved through the utilization of two primary textile technologies: blended yarn spinning and multibeam weaving **Figure 14 (c, d).** In order to enhance the evaporation efficiency of the photothermal device, a bionic fabric structure inspired by the aquatic plant Pistia has been devised with the aim of minimizing heat dissipation and maximizing the use of material. The capacity of the system is enhanced by leveraging the porous structure and gradient capillary effect of the evaporator. By positioning the photothermal component 3.2 cm above the water surface, the evaporation efficiency is significantly increased from 52.70% in its initial state to 88.70% with evaporation rate 1.50 kg $m^{-2}h^{-1}$ under the influence of 1 sun (1 kW m^{-2}). In conjunction with the affordable nature of waste carbon fiber and well-established textile technologies, the overall price of raw materials for the device is decreased to USD 3.54 m^2. This research presents potential opportunities for an economically viable and scalable method of generating steam from solar power.

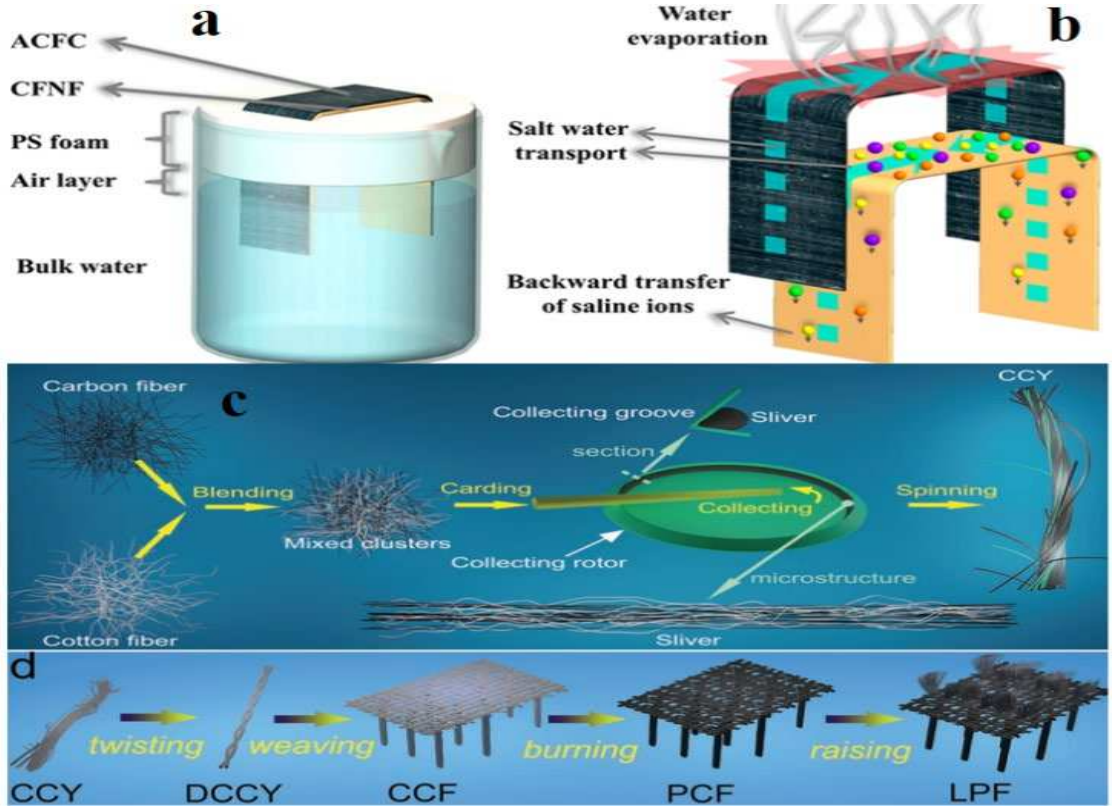

Figure 14. (a) The design of the SSG system. (b) The transportation routes of water and salt on ACFC and CFNF in ISSG [71] copy right 2019 American Chemical Society (c) The blending spinning process of carbon-cotton yarn (CCY) (d) The production process of the LPF using the CCY [73] copy right 2022 Wiley.

2.3. Electro-spun membranes:

Electro-spun membranes are commonly manufactured using the electrospinning technique, [92] it is a highly adaptable textile technique for producing flexible nano/micron fibers membranes [5,93]. It is a process that involves the application of an electric field to create fine fibers from a polymer solution or melt [54,66]. Fiber membranes produced through electrospinning exhibit controlled fiber arrangement, elevated porosity, exceptional mechanical characteristics, and a network of interconnected pores. [94]. Moreover, these fibers have diameters typically in the range of tens to

Preprints (www.preprints.org) | NOT PEER-REVIEWED | Posted: 28 December 2023 doi:10.20944/preprints202312.2214.v1

hundreds of nanometers, resulting in a high surface area-to-volume ratio and unique properties such as customizable fiber dimensions and pore architectures [55,95], rendering those promising materials for wide range of applications such as; filtration medium with elevated permeability, water treatment [96]. However, recently, numerous solar vapor generators utilizing electrospun nanofibers and nonwoven fabrics have been created within the domain of solar vapor generation [5,97]. A cost-effective, buoyant, long-lasting, and expandable evaporator has been developed, incorporating an exposed nanofiber-based dual-purpose framework to generate solar steam efficiently is designed by Gao T. et al [98]. The combined bilayer evaporator is constructed sequentially, starting from the bottom with layers of electrospun hydrophobic polyvinylidene fluoride (PVDF) nanofibers, followed by layers of hydrophilic carbon black/polyacrylonitrile (CB/PAN) composite nanofibers **Figure 15 (a, b).** The presence of a porous hydrophobic PVDF nanofiber layer can be attributed to its inherent poor thermal conductivity. This layer is a floating support and thermal barrier, mitigating irreparable heat loss. The upper layer of the composite nanofiber, consisting of hydrophilic CB/PAN, has a significant solar adsorption capacity throughout a wide range of wavelengths (250-2500 nm), reaching an impressive efficiency of 98.6%. This characteristic enables efficient conversion of solar irradiation into usable heat energy. The CP/P evaporator, when completed, demonstrates a noteworthy solar energy conversion efficiency of 82.0% and evaporation rate of 1.2 kg m^{-2} h^{-1} when subjected to 1sun illumination. The polymer-nanofiber-based evaporator, which exhibits cost-efficiency, remarkable adaptability, resilience, and capacity, shows significant potential for real-world use in water desalination and disinfection.

Using electrospinning and laser treatment processes, Chen Z. et al [60] fabricated a photothermal membrane with a three-dimensional (3D) structure. This membrane is composed of laser-induced graphene (LIG) and polyimide (PI) and exhibits significant porosity **Figure 15 (c).** 3D configuration of the LIG/PI membrane enhances the surface area available for evaporation and mitigates the energy dissipation resulting from the scattering of light. The LIG/PI membrane demonstrates a notable evaporation rate of approximately 1.42 kg m^{-2} h^{-1}, and a significant solar thermal conversion efficiency of approximately 92.55%. It exhibits long-term evaporation stability in a high-concentration saline solution under one sun illumination, thanks to incorporating an insulating layer and water flow pathways. This durable photothermal membrane has the potential to offer valuable insights for the development of interfacial evaporation systems that are both quick and efficient.

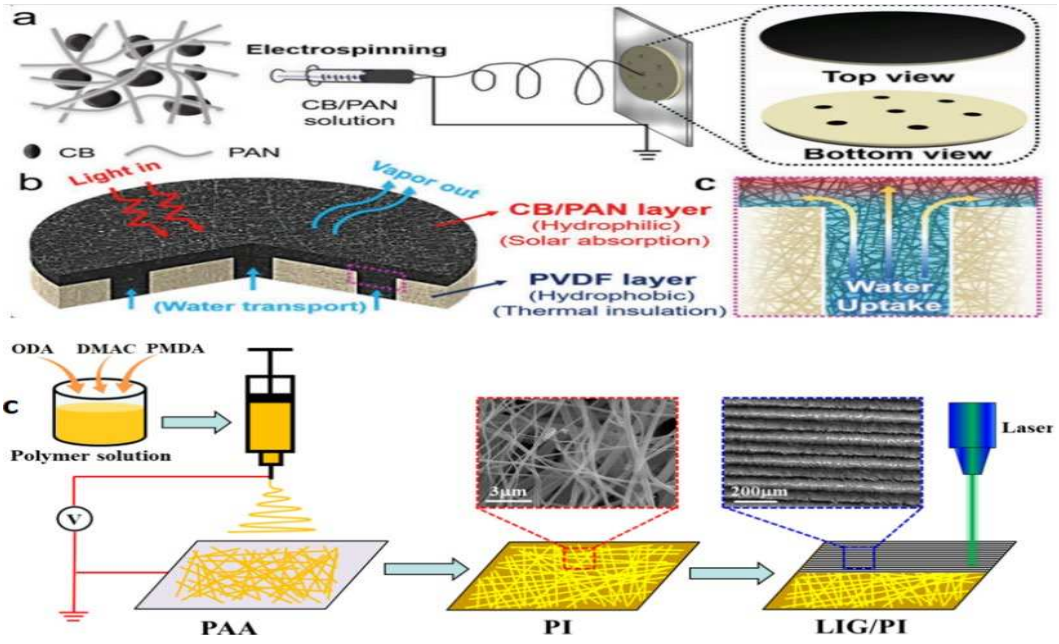

Figure 15. (a) The fabrication process and structure of the of the bilayer SSG device using an electrospinning method(b) the X-section of hydrophilic CB/PAN and hydrophobic holey PVDF layers [98] copy right 2018 WILEY (c) the design process of PI membrane and LIG/PI membrane [60] copy right 2020 American Chemical Society.

Preprints (www.preprints.org) | NOT PEER-REVIEWED | Posted: 28 December 2023 doi:10.20944/preprints202312.2214.v1

The utilization of a solution-electrospun nanofiber membrane has been recognized as a highly suitable framework for solar steam generation. This is attributed to its various advantageous characteristics, including its substantial porosity which facilitates efficient absorption of light, its significant permeability that enables rapid water transport, and its cost-effectiveness, portable nature, and exceptional adaptability, rendering it extremely useful for real-world applications [99]. However, an effective and flexible fiber membrane of silicon dioxide/carboxylated multi-walled carbon nanotube/polyacrylonitrile (SiO_2/MWCNTs-COOH/PAN) was fabricated by Qu Q. et al [100] by using electrospinning **Figure 16 (a, b)**. Subsequently, an interfacial water evaporator was constructed by affixing it onto a filter paper substrate, employing insulating polystyrene (PS) foam as the supporting substance, and utilizing cotton yarns for water conveyance. The design offers multiple benefits, including preventing heat dissipation to the bulk water and assuring high evaporation effectiveness. The composite fiber membrane demonstrated a high evaporation rate of 1.28 kg m^{-2} h^{-1} and an impressive photothermal conversion efficiency of 82.52% when exposed to 1 solar irradiation (1000 W m^{-2}). In addition, it is worth noting that the composite fiber membrane that was created exhibited remarkable stability in evaporation rate and efficiency, even after undergoing 20 consecutive evaporation cycles. Therefore, the interfacial water evaporator developed in this study shows exceptional photothermal conversion efficiency, making it a highly viable option for solar-powered saltwater desalination. Additionally, Ag nanoparticles adorned MXene nanosheets/polyacrylonitrile (Ag@MXene/PAN) nanofiber-based evaporators with a high efficiency, multipurpose, and unidirectional SSG device is fabricated by Liu H. et al [99] **Figure 16 (c)**. However, the combination of Ag nanoparticles and MXene nanosheets exhibits several advantageous properties, including enhanced broadband light absorption and heat generation and improved catalytic and antibacterial capabilities. In addition, the membrane possess the beneficial properties of elasticity and foldability, which allow for creating a three-dimensional evaporator with enhanced evaporation surface area and optimal light absorption. The developed evaporator exhibits steady evaporation rates throughout a broad range of incident angles, from 30° to 150°. Under 1 sunlight, the maximum evaporation rate approaches 2.08 kg m^{-2} h^{-1}, significantly higher than the state-of-the-art solution-electrospun nanofiber-based evaporators. The combination of structural adaptability, outstanding efficiency, and multi-functionality renders the developed nanofiber-based evaporator extremely desirable for producing clean water in practical uses.

Plasmonic silver nanoparticles (Ag NPs) as photothermal coatings and electrospun polyacrylonitrile (PAN) nanofiber membranes as substrates are utilized by lin Y. et al [101]. The diameters of Ag NPs and the light-absorption capabilities of the associated nanofiber membrane were controlled by altering the volume ratios of glucose and silver ammonia solution. Consequently, the Ag@PAN nanofiber membrane exhibited a notable light-absorption efficiency of 92.8% within the wavelength range of 280–2500 nm. Under irradiations of 1 sun the evaporation rate and evaporation efficiency were1.34 kg m^{-2} h^{-1} and 76.0, respectively. The plasmonic nanofiber membrane demonstrated sustained operational stability, as seen by its consistent solar vapor generation capability during a series of 10 cycle tests, without any observable degradation. This research establishes a foundation for the conceptualization and creation of plasmonic nanofiber membranes with the potential to function as efficient interfacial solar vapor generators. In recent study, An aerogels with a hierarchical pore structure using an environmentally friendly bonding and freeze-drying process developed by Liu Y. et al [97] by using electrospinning technique. These aerogels were composed of electrospun nanofibers made from a blend of polyacrylonitrile and carbon nanotubes (PAN/CNTs), it is developed by combining the synergistic photothermal effect of PDA and CNTs, which significantly increased light absorption efficiency, reaching 94.8%. The device demonstrated a rapid evaporation rate of 2.13 kg m^{-2} h^{-1} and a high solar-vapor conversion efficiency of 94.5% under one sun, surpassing the majority of previously published solar vapor generators based on electrospun nanofibers. The aerogel described herein offers a flexible, environmentally sustainable, and economically viable solution for producing clean water.

Preprints (www.preprints.org) | NOT PEER-REVIEWED | Posted: 28 December 2023 doi:10.20944/preprints202312.2214.v1

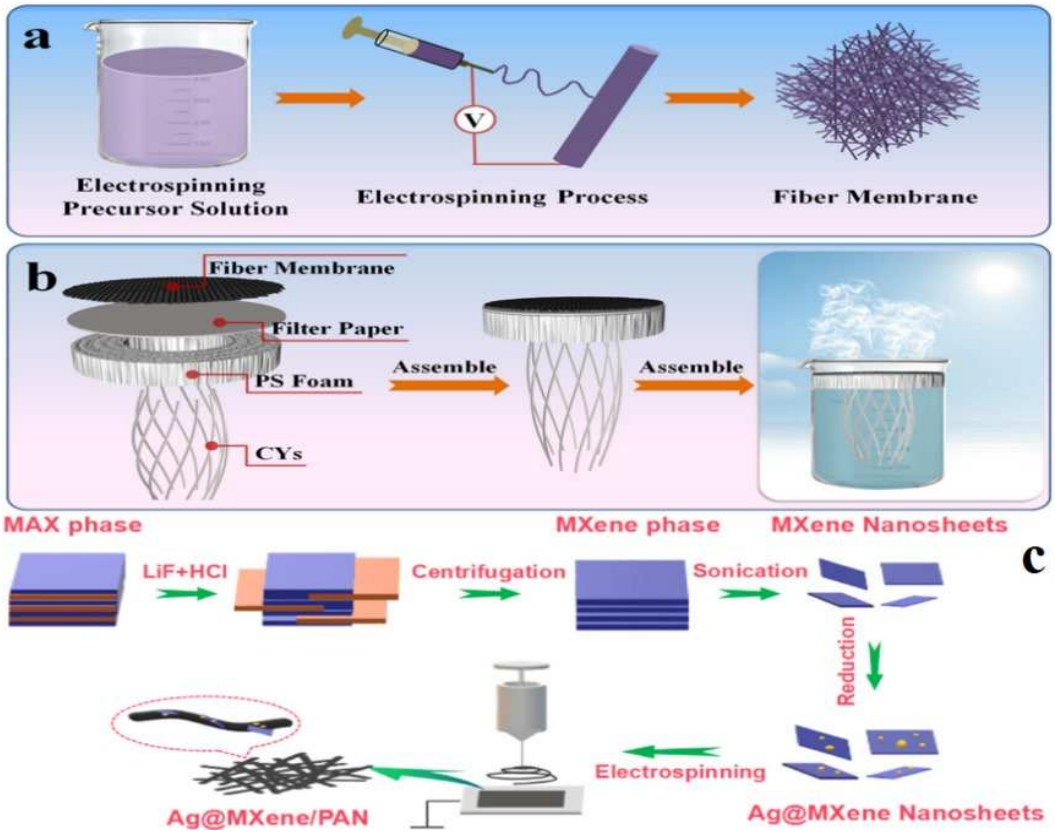

Figure 16. (a) the fabrication of (a) electrospinning fiber membranes and assembled of (b) interfacial water evaporator [100] copy right 2020 Elsevier.(c)The diagram of the design of Ag@MXene/PAN nanofiber membrane [99] copy right 2021 Elsevier.

Xu W. et al [102] studied showcases the efficacy of a foldable Janus absorber, manufactured by a sequential electrospinning process, in facilitating reliable and effective solar desalination. The distinctive architecture of Janus is leveraged to separate the processes of steam generation, namely solar absorption and water pumping, into distinct layers. The topmost layer consists of a hydrophobic coating of carbon black nanoparticles (CB) embedded in polymethylmethacrylate (PMMA), facilitating light absorption. Meanwhile, the lower layer comprises a hydrophilic polyacrylonitrile (PAN) responsible for the water-pumping mechanism. Hence, salt deposition exclusively occurs inside the hydrophilic PAN layer, facilitated by the continuous influx of water, leading to its rapid dissolution. The Janus absorber exhibits a notable level of performance, reaching 72%, which surpasses the performance of many prior absorbers. Additionally, it shows a consistent water output of 1.3 kg m^{-2} h^{-1} over 16 days under 1-sun conditions, a feat that most previous absorbers have not accomplished. The flexible Janus absorber exhibits a distinctive framework attained by an adjustable technique. This absorber is an effective, reliable, and easily transportable solar steam generator specifically designed for direct sun desalination.

The demonstration of a membrane composed of a hybrid nanofibrous hydrogel-reduced graphene oxide (NHrG) is studied by Zhang L. et al [103] by using elecrospinning technology. The results providing evidence for the existence of intermediate water within the permeable membrane through the observation of the vaporization enthalpy in relation to the saturation of the membrane. Moreover, this finding highlights the significant influence of intermediate water vaporization in reducing the overall vaporization enthalpy. The decreased enthalpy value, in conjunction with many other aspects, such as the enhanced light absorption efficiency facilitated by reduced graphene oxide (rGO) and the formation of a porous hydrophilic network produced by electrospun hydrogel nanofibers, contributed to the development of a very effective solar-driven interfacial evaporator. The NHrG membrane exhibited a maximum evaporation rate of 1.85 kg m^{-2} h^{-1}, accompanied by a

Preprints (www.preprints.org) | NOT PEER-REVIEWED | Posted: 28 December 2023 doi:10.20944/preprints202312.2214.v1

notable energy conversion efficiency of 95.4% when subjected to 1 sun irradiation. Furthermore, the evaporator demonstrated exceptional desalination efficacy when employed for the treatment of unpolluted seawater, effectively eliminating salt and heavy metal ions.

2.4. Knitting Fabrics:

Knitting is a textile production method that involves creating interlocking loops of yarn or thread using knitting needles or machines. Knitted fabrics have distinct characteristics and are widely used in various applications. However, a cost-effective and adaptable photothermal membrane (PTM) is fabricated by Wan P. et al [104] from basalt fibers derived from natural basalt by using knitting technology **Figure 17 (a, b)**. The synthesis of the basalt-fiber PTM involves the processes of fiber formation and heating. Due to its unique chemical composition and structural characteristics, the PTM exhibits exceptional durability and corrosion resistance in challenging conditions, including harsh acids, organic solvents, and alkalis. The investigation focuses on the techniques of water evaporation, with particular attention given to the floating-with-insulator model. This technique shows the least heat dissipation and the fastest rate of water evaporation. The optimization of the basalt-fiber fabric involves the processes of carbonization and vaporization. Through these processes, a vaporization rate of 1.50 $kg.m^{-2}h^{-1}$ and an energy utilization efficiency of 82.5% are attained for the evaporation of clean water. The PTM made from basalt fiber exhibits a notable resistance to efficiency degradation, allowing it to withstand hand washing for a minimum of 30 cycles. The manufacturing method's scalability enables it to cater to commercial demands effectively.

An easily manufactured, cost-effective, and highly reliable solar-driven evaporator is fabricated by Yang Y. et al [8] by utilizing a dyed cotton towel with a hollow conical shape. After the dyeing process **Figure 17 (c)**, the reactive dye molecules undergo diffusion into the cotton fabric and establish robust covalent bonds with the fibers. This results in the secure attachment of light-absorbing components onto the substrate. Utilizing a looping pile architecture in towels and an ordered arrangement in yarns facilitates the expansion of the evaporator's surface area. The cotton towel's hollowed cylindrical structure demonstrates a notable capacity to mitigate heat dissipation to the surrounding environment while maintaining its ability to absorb light. The 3D vapor generator indicates an evaporation rate of 1.40 and 1.27 kg m^{-2} h^{-1} for pure and saline water. Moreover, it offers a dependable approach for addressing practical water sources, including saltwater and dyeing wastewater. Hence, a cost-effective water evaporation system powered by solar energy presents a supplementary method for achieving optimal vapor generation and water purification in real-world scenarios.

Preprints (www.preprints.org) | NOT PEER-REVIEWED | Posted: 28 December 2023 doi:10.20944/preprints202312.2214.v1

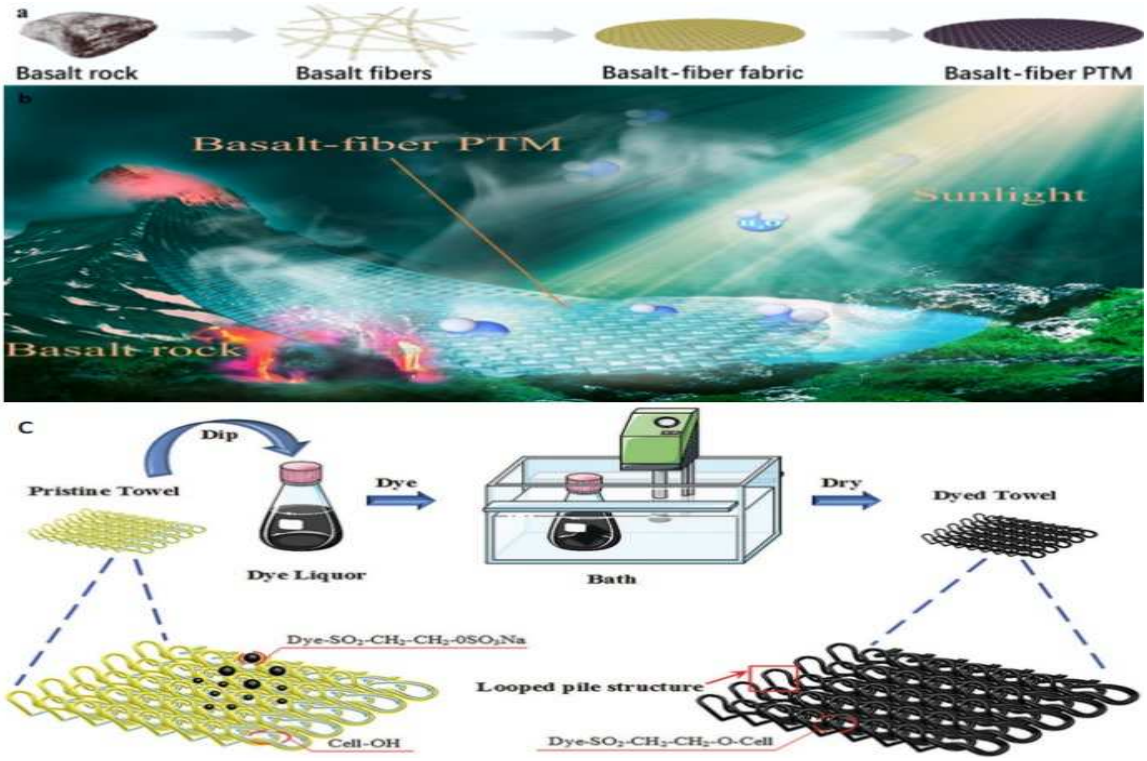

Figure 17. (a) A diagram depicting the procedure for the fabrication of the basalt-fiber (PTM) (b)The design of the basalt-fiber PTM on photothermal evaporation system [104] copy right 2021 Elsevier. (c) Diagram of the dyeing steps [8] copy right 2019 WILEY.

Wang F. et al [47] developed an innovative solar steam generation system utilizing a hollow spacer fabric (HSF) that has been modified by incorporating chitosan and applying a reduced graphene oxide coating onto its outermost layer. The improved BHSF exhibits enhanced efficiency in terms of water transport and mechanical properties due to its porous textile fabric structure, which provides superior thermal insulation. It demonstrates an elastic modulus of up to 733 kPa at a strain of 70% and a low thermal conductivity of 0.08 W m^{-1} K^{-1}. When subjected to sun irradiation with a power density of 1 kW/m^{-2}, this particular solar generator exhibits an evaporation efficiency of 86% with an evaporation rate of 1.44 kg m^{-2} h^{-1}. The improved BHSF exhibits exceptional resistance to salt, particularly in high saline solutions, due to its distinctive cylindrical structure and the presence of a well-aligned array of large channels measuring 2 mm in size. This distinctive design provides extra pathways with minimal tortuosity, facilitating efficient evaporation. BHSF exhibits promising prospects for the large-scale production of a cost-effective solar still. This solar still possesses exceptional mechanical versatility, physicochemical durability, and a high solar energy conversion efficiency. These attributes make it suitable for various uses, such as power generation, desalination, and steam sterilization.

Pursuing an ecologically sustainable method for acquiring cellulose nanofiber and fabricating an evaporator based on aerogel represents a pragmatic necessity. However, He M. et al [105] fabricated a novel cellulose hybrid aerogel ISSG that is both stable and green from waste cotton fibers The aerogel composed of polyethyleneimine cross-linked carbon nanotubes and cellulose nanofibers (PEI@CNTs/CNFs), it shows a notable solar steam generation rate of 1.9 kg m^{-2} h^{-1} with a light a vapor conversion rate of 91.4% when exposed to 1 sun irradiation. Furthermore, the evaporator can ensure consistent and enduring efficiency for solar steam generation even after undergoing extensive long-term testing. In addition, the device can treat many types of wastewater, such as dye sewage, toxic ion wastewater, and seawater. The characteristics above of the cellulose-based composite aerogel provide a highly effective method for solar-powered water filtration, regeneration, and desalination. Regeneration cellulose aerogels (CAs) functionalized with polydopamine (PDA) have been

Preprints (www.preprints.org) | NOT PEER-REVIEWED | Posted: 28 December 2023 doi:10.20944/preprints202312.2214.v1

developed by Liu H. et al [28] by using an environmentally friendly and practical approach to facilitate the production of clean water. By initiating the polymerization of PDA on the surface, a material known for its remarkable photothermal conversion capabilities and water-purifying properties, the result demonstrates a notable light absorption efficiency of 96.5% and an evaporation rate of 2.74 kg m^{-2} h^{-1} under 1 sun irradiation. In the context of solar steam production, it has been observed that a solar steam generator with an increasing height can absorb energy from the surrounding atmosphere, hence enhancing the process of vapor creation. Renewable cellulose-based aerogels have inherent characteristics that facilitate effective water evaporation. These attributes, together with their cost-effectiveness and recyclability, hold significant potential in mitigating both energy consumption and the environmental impact associated with cotton fabric.

3. Salt rejection and accumulation in textile materials based ISSG system:

The continuous process of saltwater evaporation results in the deposition of salt on the surface of photothermal conversion materials. This salt buildup has the potential to obstruct the steam channels and subsequently diminish the rate of water evaporation. The avoidance of salt accumulation on solar-driven evaporators is a crucial consideration in their practical implementation [106]. However, salt accumulation is frequently seen in sun desalination operations, particularly in brine with high salt levels. The presence of precipitated salt has the potential to obstruct water pathways, impede the passage of vapor through escape channels, diminish the capacity of the evaporation surface to absorb light, and thus lead to decreased effectiveness in evaporation while operating continuously in saline water [38]. However, the accumulation of salt on the absorbers during the process of desalination is a significant challenge, as it has the potential to degrade and disrupt the ongoing production of steam. Several effective solutions have been described in the literature to mitigate salt buildup. These method can be categorized into two main types: hydrophilic and hydrophobic designs, as well as contactless architectures. The hydrophilic design incorporates an extra water supply channel to facilitate the improvement of fluid convection. This convection process effectively dilutes the concentrated brine that is generated within the absorbers [46,75].

Recently, numerous meticulously planned buildings have been documented with the aim of mitigating the issue associated with surface salt precipitation, these constructions achieve this by using salt-rejecting photothermal devices that facilitate the dispersion of collected salts back to the source water [107]. The removal of solid salts from membranes can be achieved through washing. However, it should be noted that certain photothermal membranes, including fabrics, cellulose membrane and aerogel, are susceptible to damage when subjected to the washing process [38]. This is primarily attributed to the exfoliation of nanoparticles and the lack of sufficiently big micronized channels. In order to enhance the efficiency of washing and regeneration processes, it is imperative to focus on the development of innovative photothermal membranes that possess substantial microsized channels and are resistant to potential exfoliation of the photothermal nanomaterials [79].

Table 1 presents a summary of the outcomes and outstanding features of textile materials-based ISSG devices, including evaporation rate and evaporation efficiency when subjected to solar irradiation. However, due to the unique properties of the textile materials, such as thinness, lightweight nature, flexibility, comfort, porous nature, water transfer and evaporation, large surface area, and permeability. Generally, the listed ISSG textile-based devices showed an outstanding evaporation efficiency ranging from 80%- 98%, which is very competitive compared to that of many other ISSG systems. The evaporation rate is in the range of 1.18-2.32 kg $m^{-2}h^{-1}$, which is in the acceptable range of the high-performance ISSG devices reported in the literature. Among the studied systems, the vertical polypyrrole nanowires-coated fabric ISSG device demonstrated a significantly higher evaporation efficiency of 98.56% with an unparalleled evaporation rate of 2.32 kg $m^{-2}h^{-1}$ which is the highest compared with the other devices reported in the literature. On the other hand, MWCNTs -COOH/cotton fabric showed a relatively high evaporation efficiency of 86.0 1% with the lowest evaporation rate of 1.18 kg $m^{-2}h^{-1}$.

Preprints (www.preprints.org) | NOT PEER-REVIEWED | Posted: 28 December 2023 doi:10.20944/preprints202312.2214.v1

Table 1. The performance of textile materials-based ISSG devices:.

Textile Material	Materials	Efficiency (%) Under 1 sun	Evaporation rate (kg m^{-2} h^{-1})	Ref.
Woven fabrics				
	PDA/PPy nanofibers/ flax fabric	87.40	1.37	[45]
	carbon fiber/cotton yarns	83.70	1.87	[75]
	MXene/ PET fabric	80.00	1.22	[74]
	Grapheme oxide /spacer fabric	86.00	1.43	[47]
	VPPyNWs-fabric	98.56	2.32	[81]
	CB/SA/ramie fabric	96.60	1.81	[17]
	CNTs/cotton fabrics	95.70	1.59	[34]
	MXene/CNT/Cotton fabric	88.20	1.35	[58]
	carbon black/cotton fabric	88.90	1.33	[53]
	Cs_xWO_3 ink/cotton fabric	86.80	1.56	[33]
	Candle soot/ Linen fabric	90.00	1.44	[31]
	Cu/polyester textile	88.00	1.52	[82]
	MU/PAN textile	89.20	1.36	[83]
	Nafion coating/(cotton cloth-NCC)	89.90	1.52	[85]
	Polyester/cotton Janus fabric	86.30	1.37	[84]
	polypyrrole fabric/PSHF	91.68	1.49	[108]
	TiO_2 nanorods/Carbon Fabric	93.00	1.42	[42]
	PPy/cotton fabric	82.99	1.20	[72]
	carbon fiber cloth/PAN fiber cloth	93.70	1.43	[86]
	RGO/cotton fabric	N/A	1.47	[70]
	Au-CNTs /cotton fabric	N/A	2.19	[24]
	MXene/CNTs/cotton fabric	88.20	1.35	[58]
	MXene/cotton fabric	83.10	1.38	[69]
	MWCNTs -COOH/ cotton fabric	86.0 1	1.18	[21]
	PEGylated MoS_2/cotton fabric	80.50	1.30	[109]
	PPy/cotton fabric	N/A	1.54	[88]
	Carbon/cotton composite fabrics	82.00	1.25	[87]
	Polyaniline/cotton fabrics	89.90	1.94	[110]
	Janus ink/urushiol cotton fabric	94.30	1.64	[89]
	Polypyrrole/Janus cotton fabric	91.00	1.45	[111]
	Polyacrylonitrile/waste carbon fiber	88.70	1.50	[73]
	Graphene oxide/composite Tencel (GOT) fabric	90.40	1.33	[90]
	(Ag NPs)/cotton fabric	91.00	1.66	[112]

Preprints (www.preprints.org) | NOT PEER-REVIEWED | Posted: 28 December 2023 doi:10.20944/preprints202312.2214.v1

Non-woven fabrics				
	PDA/CB@PP non-woven fabric	91.50	1.68	[30]
	CNT/ polyacrylonitrile nonwoven fabrics	90.80	1.44	[79]
	PP/PE nonwoven/ MWCNTs.	89.70	1.44	[37]
	carbon black/ nylon fabric	83.00	1.24	[41]
	Carbon fiber/Cotton fiber nonwoven fabric	93.30	1.59	[71]
	MnCDs@PPy/non-woven cotton fabric	96.40	1.68	[113]
Electro-spun membranes				
	CB/PAN//PVDF composite layer	82.00	1.20	[98]
	Graphene/polyimide LIG/PI membrane	92.55	1.42	[60]
	PAN/CNTs nanofiber	94.50	2.13	[97]
	CNP/PCL nanofiber composites	N/A	1.95	[114]
	CNT/PCL nanofiber composites	N/A	2.00	[114]
	FIP-PZ/MOF fabrics	94.20	1.50	[115]
	Ag@MXene/PAN nanofiber membrane	92.40	2.08	[99]
	Ag@PAN nanofiber membrane	76.00	1.34	[101]
	SiO_2/MWCNTs-COOH/PAN fiber membrane	82.52	1.28	[100]
	GO/PVA EFMs membrane	94.20	1.42	[5]
	CNFs/PAN/TPA nanofibrous membrane	89.50	1.36	[16]
	CNT/PVDF/PVP nanofiber mats	86.10	1.37	[38]
	Co_3S_4HP/PAN membrane	86.50	1.26	[116]
	CNTs@SiO_2 Nanofibrous Aerogels	98.00	1.50	[11]
	rGO/PAN membrane	89.40	1.46	[93]
	CB/PAN membrane	72.00	1.30	[102]
	rGO/NHrG membrane	95.40	1.85	[103]
	GO/PVA EFMs nanofiber mats	90.00	1.40	[5]
	Carbonized ultrafine PAN fibers	81.71	1.33	[92]
	Chinese ink/PLA fibrous mat	81.00	1.29	[95]
Knitting fabrics				
	Carbonized basalt-fiber fabric	82.50	1.50	[104]
	3D dyed black cotton towel	72.00	1.40	[8]
	Chitosan/graphene oxide /3D spacer fabric	86.00	1.44	[47]
	PEI@CNTs/waste cotton fabric	91.40	1.90	[105]

N/A: data is not available.

Preprints (www.preprints.org) | NOT PEER-REVIEWED | Posted: 28 December 2023 doi:10.20944/preprints202312.2214.v1

4. The drawbacks and the challenges of textile materials-based ISSG devices:

The efficiency of solar-driven evaporation systems can be influenced by factors such as weather conditions, temperature, and the availability of sunlight. Additionally, the scalability and productivity of solar-driven evaporation systems need to be carefully considered to meet the demands of large-scale desalination projects. The following criteria are the most significantly impede their potential for future industrial applications [75].

1. Scaling up: Many of the current solar interfacial evaporation techniques are still at the laboratory or small-scale prototype stage. Scaling up the technology to an industrial level presents challenges in terms of maintaining efficiency, cost-effectiveness, and system stability. Further research and development are needed to optimize the design and manufacturing processes for large-scale implementation.
2. Adaptability: Solar interfacial evaporation systems need to be adaptable to various environmental conditions and water sources. Factors such as solar intensity, temperature variations, water quality, and impurities can affect the performance of the system. Developing adaptable and robust systems that can operate effectively under different conditions is essential.
3. Stability and durability: Solar interfacial evaporation systems operate in harsh environments, including exposure to sunlight, saltwater, and other contaminants. The materials used in these systems should be stable, durable, and resistant to degradation over extended periods. Ensuring long-term stability is crucial for the practical and reliable operation of the technology.
4. Integration with existing infrastructure: To facilitate widespread adoption, solar interfacial evaporation systems need to be compatible with existing water treatment and distribution infrastructure. Integration with existing systems, such as storage and distribution networks, would enable seamless implementation and utilization of the produced freshwater.

Addressing these limitations requires ongoing research and development efforts, interdisciplinary collaboration, and technological advancements. With continued progress, it is possible to overcome these challenges and unlock the full potential of solar interfacial evaporation for future industrial applications in freshwater production.

5. Future Prospects and Recommendations:

The utilization of textile materials in solar steam generation exhibits favorable future possibilities. Textile substances possess distinct benefits, including adaptability, lightweight, expansion, and affordability, rendering them well-suited for solar steam-generating technologies. Below are some potential uses of textile materials in this domain:

1. Solar steam generation can be employed for desalination, wherein saltwater or brackish water is transformed into potable water via evaporation and condensation. Textile materials, such as woven or knitted with appropriate surface coatings, can be highly effective solar absorbers for capturing solar energy and producing steam for desalination. Due to their adaptability and capacity for expansion, they are well-suited for solar desalination processes on a wide scale.
2. Textile materials can be employed in the production of solar steam generation systems. Textiles featuring sophisticated coatings or fibers modified for specific functions can be integral in constructing solar collectors, steam chambers, or heat transfer systems. Integrating textile manufacturing experience can improve the efficiency and performance of solar steam generation systems.
3. Further gains can be achieved by ongoing research and innovation in textile materials and their utilization in solar steam generation. This encompasses the creation of innovative textile architectures, surface treatments, or substances with heightened sun absorption capabilities, enhanced heat conduction attributes, and augmented longevity. Textile-based solar steam-generating methods can be further enhanced by advancements in nanotechnology, intelligent fabrics, and improved manufacturing techniques.
4. It is crucial to acknowledge that textile materials present promising opportunities for generating solar steam. However, there remain obstacles to address, including the need to enhance textile-based systems' efficiency, longevity, and adaptability. Additionally, ensuring stability over time in harsh environments and effectively integrating these systems into current structures pose significant considerations. Nevertheless, with continuous research and improvement endeavors,

Preprints (www.preprints.org) | NOT PEER-REVIEWED | Posted: 28 December 2023 doi:10.20944/preprints202312.2214.v1

the utilization of textile materials in generating steam from solar energy is expected to broaden. This will aid in providing sustainable energy solutions and tackling worldwide issues related to water shortages, energy accessibility, and environmental sustainability.

6. Conclusions:

Solar interfacial evaporation has emerged as a technology that is receiving considerable interest due to its potential to effectively mitigate the issue of worldwide freshwater scarcity. There are many attractive characteristics available in textile materials. They are very appropriate for a wide range of products and uses because of their thinness, lightweight nature, flexibility, comfort, porous nature, water transfer and evaporation, large surface area, and permeability. However, recently, the use of textile materials in ISSG showed encouraging results in a variety of applications for wastewater purification and desalination. This comprehensive review examines several textile materials, including woven, nonwoven, knitted textiles, and electro-spun membranes and explores these materials' distinct roles and advantages in purifying wastewater and desalinating water within the ISSG. Moreover, it is also highlights the difficulties associated with the advancement of using textile materials in ISSG systems for wastewater purification.

Acknowledgments: This study was supported by Key Research and Development Program of Hubei Province (No.2022ACA002).

References

1. Yan, J.; Su, Q.; Xiao, W.; Wu, Z.; Chen, L.; Tang, L.; Zheng, N.; Gao, J.; Xue, H., A review of nanofiber membranes for solar interface evaporation. Desalination. **531**, 2022, 115686.
2. Li, H.; Wen, H.; Li, J.; Huang, J.; Wang, D.; Tang, B.Z., Doping AIE Photothermal Molecule into All-Fiber Aerogel with Self-Pumping Water Function for Efficiency Solar Steam Generation. ACS Appl. Mater. Interfaces. **12**, 2020, 26033-26040.
3. Tessema, A.A.; Wu, C.-M.; Motora, K.G.; Naseem, S., Highly-efficient and salt-resistant CsxWO3@g-C3N4/PVDF fiber membranes for interfacial water evaporation, desalination, and sewage treatment. Compos. Sci. Technol. **211**, 2021, 108865.
4. Gao, Z.; Yang, H.; Li, J.; Kang, L.; Wang, L.; Wu, J.; Guo, S., Simultaneous evaporation and decontamination of water on a novel membrane under simulated solar light irradiation. Appl. Catal. B **267**, 2020, 118695.
5. Guo, X.; Gao, H.; Wang, S.; Yin, L.; Dai, Y., Scalable, flexible and reusable graphene oxide-functionalized electrospun nanofibrous membrane for solar photothermal desalination. Desalination. **488**, 2020, 114535.
6. Wei, Z.; Wang, J.; Guo, S.; Tan, S.C., Towards highly salt-rejecting solar interfacial evaporation: Photothermal materials selection, structural designs, and energy management. Nano Research Energy. **1**, 2022, 9120014.
7. Lu, F.; Wu, S.-L.; Quan, L.-N.; Zhong, Z.-H.; Yang, H.-C.; Xue, M., Twisting two-dimensional photothermal sponges for boosting solar steam generation. J. Chem. Eng. **474**, 2023, 145747.
8. Yang, Y.; Sui, Y.; Cai, Z.; Xu, B., Low-Cost and High-Efficiency Solar-Driven Vapor Generation Using a 3D Dyed Cotton Towel. Global chall. **3**, 2019, 1900004.
9. Mei, T.; Chen, J.; Zhao, Q.; Wang, D., Nanofibrous aerogels with vertically aligned microchannels for efficient solar steam generation. ACS Appl. Mater. Interfaces. **12**, 2020, 42686-42695.
10. Dong, X.; Si, Y.; Chen, C.; Ding, B.; Deng, H., Reed Leaves Inspired Silica Nanofibrous Aerogels with Parallel-Arranged Vessels for Salt-Resistant Solar Desalination. ACS Nano. **15**, 2021, 12256-12266.
11. Dong, X.; Cao, L.; Si, Y.; Ding, B.; Deng, H., Cellular Structured CNTs@SiO2 Nanofibrous Aerogels with Vertically Aligned Vessels for Salt-Resistant Solar Desalination. Adv. Mater. **32**, 2020, 1908269.
12. Zhang, W.; Xia, Y.; Wen, Z.; Han, W.; Wang, S.; Cao, Y.; He, R.X.; Liu, Y.; Chen, B., Enhanced adsorption-based atmospheric water harvesting using a photothermal cotton rod for freshwater production in cold climates. RSC Adv. **11**, 2021, 35695-35702.
13. Chen, C.; Wang, M.; Chen, X.; Chen, X.; Fu, Q.; Deng, H., Recent progress in solar photothermal steam technology for water purification and energy utilization. J. Chem. Eng. **448**, 2022, 137603.
14. Zhang, Y.; Wang, F.; Yu, Y.; Wu, J.; Cai, Y.; Shi, J.; Morikawa, H.; Zhu, C., Multi-bioinspired hierarchical integrated hydrogel for passive fog harvesting and solar-driven seawater desalination. J. Chem. Eng. **466**, 2023, 143330.
15. Liu, X.; Mishra, D.D.; Wang, X.; Peng, H.; Hu, C., Towards highly efficient solar-driven interfacial evaporation for desalination. J. Mater. Chem. A. **8**, 2020, 17907-17937.

Preprints (www.preprints.org) | NOT PEER-REVIEWED | Posted: 28 December 2023 doi:10.20944/preprints202312.2214.v1

16. Yan, J.; Xiao, W.; Chen, L.; Wu, Z.; Gao, J.; Xue, H., Superhydrophilic carbon nanofiber membrane with a hierarchically macro/meso porous structure for high performance solar steam generators. Desalination. **516**, 2021, 115224.
17. Gao, C.; Zhu, J.; Bai, Z.; Lin, Z.; Guo, J., Novel ramie fabric-based draping evaporator for tunable water supply and highly efficient solar desalination. ACS Appl. Mater. Interfaces. **13**, 2021, 7200-7207.
18. Wang, L.; Ma, Y.; Yang, G.; Li, X.; Liu, D.; Qin, S.; Lei, W., Asymmetric solar evaporator with salt-resistance capability for freshwater and energy generation. J. Chem. Eng. **472**, 2023, 144761.
19. Wu, S.-L.; Chen, H.; Wang, H.-L.; Chen, X.; Yang, H.-C.; Darling, S.B., Solar-driven evaporators for water treatment: challenges and opportunities. Environmental Science: Environ. Sci. Water Res. **7**, 2021, 24-39.
20. Xiao, Y.; Wang, X.; Li, C.; Peng, H.; Zhang, T.; Ye, M., A salt-rejecting solar evaporator for continuous steam generation. J. Environ. Chem. Eng. **9**, 2021, 105010.
21. Qi, Q.; Wang, Y.; Wang, W.; Ding, X.; Yu, D., High-efficiency solar evaporator prepared by one-step carbon nanotubes loading on cotton fabric toward water purification. Sci. Total Environ. **698**, 2020, 134136.
22. Wu, Y.; Ma, J.; Zang, S.; Zhou, W.; Wang, Z.; Han, M.; Osman, S.M.; Wang, C.; Yamauchi, Y.; You, J., et al., Multifunctional composite membranes for interfacial solar steam and electricity generation. J. Chem. Eng. **472**, 2023, 144600.
23. Huang, H.; Zhao, L.; Yu, Q.; Lin, P.; Xu, J.; Yin, X.; Chen, S.; Wang, H.; Wang, L., Flexible and Highly Efficient Bilayer Photothermal Paper for Water Desalination and Purification: Self-Floating, Rapid Water Transport, and Localized Heat. ACS Appl. Mater. Interfaces. **12**, 2020, 11204-11213.
24. Zhang, C.; Xiao, P.; Ni, F.; Yang, Y.; Gu, J.; Zhang, L.; Xia, J.; Huang, Y.; Wang, W.; Chen, T., Programmable Interface Asymmetric Integration of Carbon Nanotubes and Gold Nanoparticles toward Flexible, Configurable, and Surface-Enhanced Raman Scattering Active All-In-One Solar-Driven Evaporators. Energy Technol. **7**, 2019, 1900787.
25. Zhao, S.; Zhang, X.; Wei, G.; Su, Z.J.C.E.J., All-weather photothermal-electrothermal integrated system for efficient solar steam generation. J. Chem. Eng. **458**, 2023, 141520.
26. Li, W.; Tian, X.; Li, X.; Liu, J.; Li, C.; Feng, X.; Shu, C.; Yu, Z.-Z., An environmental energy-enhanced solar steam evaporator derived from MXene-decorated cellulose acetate cigarette filter with ultrahigh solar steam generation efficiency. J. Colloid Interface Sci. **606**, 2022, 748-757.
27. Jiang, M.; Shen, Q.; Zhang, J.; An, S.; Ma, S.; Tao, P.; Song, C.; Fu, B.; Wang, J.; Deng, T., et al., Bioinspired Temperature Regulation in Interfacial Evaporation. Adv. Funct. Mater. **30**, 2020, 1910481.
28. Liu, H.; Alam, M.K.; He, M.; Liu, Y.; Wang, L.; Qin, X.; Yu, J., Sustainable Cellulose Aerogel from Waste Cotton Fabric for High-Performance Solar Steam Generation. ACS Appl. Mater. Interfaces. **13**, 2021, 49860-49867.
29. Yuan, J.; Lei, X.; Yi, C.; Jiang, H.; Liu, F.; Cheng, G.J., 3D-printed hierarchical porous cellulose/alginate/carbon black hydrogel for high-efficiency solar steam generation. J. Chem. Eng. **430**, 2022, 132765.
30. Sun, S.; Sun, B.; Wang, Y.; Antwi-Afari, M.F.; Mi, H.-Y.; Guo, Z.; Liu, C.; Shen, C., Carbon black and polydopamine modified non-woven fabric enabling efficient solar steam generation towards seawater desalination and wastewater purification. Sep. Purif. Technol. **278**, 2021, 119621.
31. Song, L.; Mu, P.; Geng, L.; Wang, Q.; Li, J., A Novel Salt-Rejecting Linen Fabric-Based Solar Evaporator for Stable and Efficient Water Desalination under Highly Saline Water. ACS Sustain. Chem. Eng. **8**, 2020, 11845-11852.
32. Wu, X.; Robson, M.E.; Phelps, J.L.; Tan, J.S.; Shao, B.; Owens, G.; Xu, H., A flexible photothermal cotton-CuS nanocage-agarose aerogel towards portable solar steam generation. Nano Energy. **56**, 2019, 708-715.
33. Liu, Z.; Zhong, Q.; Wu, N.; Zhou, H.; Wang, L.; Zhu, L.; Jiang, N.; Zhu, B.; Chen, Z.; Zhu, M., Vertically symmetrical evaporator based on photothermal fabrics for efficient continuous desalination through inversion strategy. Desalination. **509**, 2021, 115072.
34. Kou, H.; Liu, Z.; Zhu, B.; Macharia, D.K.; Ahmed, S.; Wu, B.; Zhu, M.; Liu, X.; Chen, Z., Recyclable CNT-coupled cotton fabrics for low-cost and efficient desalination of seawater under sunlight. Desalination. **462**, 2019, 29-38.
35. Li, H.; Yan, Z.; Li, Y.; Hong, W., Latest development in salt removal from solar-driven interfacial saline water evaporators: Advanced strategies and challenges. Water Res. **177**, 2020, 115770.
36. Cao, P.; Yuan, P.; Zhao, L.; Yang, Z.; Zhang, Y.; Wang, B.; Cao, Y.; Yong, Z.; Niu, Y.; Zhang, J., et al., Plant-inspired multi-environmentally adaptive, flexible, and washable solar steam generation fabric. J. Chem. Eng. **471**, 2023, 144286.
37. Zhu, Y.; Tian, G.; Liu, Y.; Li, H.; Zhang, P.; Zhan, L.; Gao, R.; Huang, C., Low-cost, unsinkable, and highly efficient solar evaporators based on coating MWCNTs on nonwovens with unidirectional water-transfer. Adv. Sci. **8**, 2021, 2101727.
38. Liang, P.; Liu, S.; Ding, Y.; Wen, X.; Wang, K.; Shao, C.; Hong, X.; Liu, Y., A self-floating electrospun nanofiber mat for continuously high-efficiency solar desalination. Chemosphere. **280**, 2021, 130719.

Preprints (www.preprints.org) | NOT PEER-REVIEWED | Posted: 28 December 2023 doi:10.20944/preprints202312.2214.v1

39. Wu, X.; Wu, Z.; Wang, Y.; Gao, T.; Li, Q.; Xu, H., All-Cold Evaporation under One Sun with Zero Energy Loss by Using a Heatsink Inspired Solar Evaporator. Adv. Sci. **8**, 2021, 2002501.
40. Li, X.; Yao, Z.; Wang, J.; Li, D.; Yu, K.; Jiang, Z., A Novel Flake-like Cu7S4 Solar Absorber for High-Performance Large-Scale Water Evaporation. ACS Appl. Energy Mater. **2**, 2019, 5154-5161.
41. Jin, Y.; Chang, J.; Shi, Y.; Shi, L.; Hong, S.; Wang, P., A highly flexible and washable nonwoven photothermal cloth for efficient and practical solar steam generation. J. Mater. Chem. A. **6**, 2018, 7942-7949.
42. Higgins, M.W.; Shakeel Rahmaan, A.R.; Devarapalli, R.R.; Shelke, M.V.; Jha, N., Carbon fabric based solar steam generation for waste water treatment. Sol. Energy . **159**, 2018, 800-810.
43. Jia, J.; Liang, W.; Sun, H.; Zhu, Z.; Wang, C.; Li, A., Fabrication of bilayered attapulgite for solar steam generation with high conversion efficiency. J. Chem. Eng. **361**, 2019, 999-1006.
44. Zhao, X.; Liu, C., Enhanced solar evaporation efficiency based on the inserted preheating zone of silver nanowires. Sol. Energy . **195**, 2020, 304-309.
45. Li, Y.; Fan, J.; Wang, R.; Shou, W.; Wang, L.; Liu, Y., 3D tree-shaped hierarchical flax fabric for highly efficient solar steam generation. J. Mater. Chem. A. **9**, 2021, 2248-2258.
46. Chen, C.; Kuang, Y.; Hu, L., Challenges and opportunities for solar evaporation. Joule. **3**, 2019, 683-718.
47. Wang, F.; Wei, D.; Li, Y.; Chen, T.; Mu, P.; Sun, H.; Zhu, Z.; Liang, W.; Li, A., Chitosan/reduced graphene oxide-modified spacer fabric as a salt-resistant solar absorber for efficient solar steam generation. J. Mater. Chem. A. **7**, 2019, 18311-18317.
48. Li, H.; He, Y.; Hu, Y.; Wang, X., Commercially Available Activated Carbon Fiber Felt Enables Efficient Solar Steam Generation. ACS Appl. Mater. Interfaces. **10**, 2018, 9362-9368.
49. Zhang, L.-Z.; Li, G.-P., Energy and economic analysis of a hollow fiber membrane-based desalination system driven by solar energy. Desalination. **404**, 2017, 200-214.
50. Dao, V.D.; Choi, H.S., Carbon-based sunlight absorbers in solar-driven steam generation devices. Global chall. **2**, 2018, 1700094.
51. Li, T.; Fang, Q.; Xi, X.; Chen, Y.; Liu, F., Ultra-robust carbon fibers for multi-media purification via solar-evaporation. J. Mater. Chem. A. **7**, 2019, 586-593.
52. Meng, X.; Xu, W.; Li, Z.; Yang, J.; Zhao, J.; Zou, X.; Sun, Y.; Dai, Y., Coupling of hierarchical Al 2 O 3/TiO 2 nanofibers into 3D photothermal aerogels toward simultaneous water evaporation and purification. Adv. Fiber Mater. **2**, 2020, 93-104.
53. Li, Y.; Jin, X.; Zheng, Y.; Li, W.; Zheng, F.; Wang, W.; Lin, T.; Zhu, Z., Tunable Water Delivery in Carbon-Coated Fabrics for High-Efficiency Solar Vapor Generation. ACS Appl. Mater. Interfaces. **11**, 2019, 46938-46946.
54. Ge, C.; Xu, D.; Du, H.; Chen, Z.; Chen, J.; Shen, Z.; Xu, W.; Zhang, Q.; Fang, J., Recent advances in fibrous materials for interfacial solar steam generation. Adv. Fiber Mater. **5**, 2023, 791-818.
55. Wu, T.; Li, H.; Xie, M.; Shen, S.; Wang, W.; Zhao, M.; Mo, X.; Xia, Y., Incorporation of gold nanocages into electrospun nanofibers for efficient water evaporation through photothermal heating. Mater. Today Energy **12**, 2019, 129-135.
56. Chen, M.; Wu, Y.; Song, W.; Mo, Y.; Lin, X.; He, Q.; Guo, B., Plasmonic nanoparticle-embedded poly (p-phenylene benzobisoxazole) nanofibrous composite films for solar steam generation. Nanoscale. **10**, 2018, 6186-6193.
57. Lin, X.; Yang, M.; Hong, W.; Yu, D.; Chen, X., Commercial Fiber Products Derived Free-Standing Porous Carbonized-Membranes for Highly Efficient Solar Steam Generation. Front. Mater. Sci. **5**, 2018.
58. Wang, Y.; Qi, Q.; Fan, J.; Wang, W.; Yu, D., Simple and robust MXene/carbon nanotubes/cotton fabrics for textile wastewater purification via solar-driven interfacial water evaporation. Sep. Purif. Technol. **254**, 2021, 117615.
59. Zhang, C.; Yuan, B.; Liang, Y.; Yang, L.; Bai, L.; Yang, H.; Wei, D.; Wang, F.; Wang, Q.; Wang, W., Carbon nanofibers enhanced solar steam generation device based on loofah biomass for water purification. Mater. Chem. Phys. **258**, 2021, 123998.
60. Chen, Z.; Li, Q.; Chen, X., Porous Graphene/Polyimide Membrane with a Three-Dimensional Architecture for Rapid and Efficient Solar Desalination via Interfacial Evaporation. ACS Sustain. Chem. Eng. **8**, 2020, 13850-13858.
61. Lin, Y.; Xu, H.; Shan, X.; Di, Y.; Zhao, A.; Hu, Y.; Gan, Z., Solar steam generation based on the photothermal effect: from designs to applications, and beyond. J. Mater. Chem. A. **7**, 2019, 19203-19227.
62. Liu, C.; Yin, Z.; Hou, Y.; Yin, C.; Yin, Z., Overview of Solar Steam Devices from Materials and Structures. Polymers. **15**, 2023, 2742.
63. Zhong, J.; Huang, C.; Wu, D.; Lin, Z., Influence factors of the evaporation rate of a solar steam generation system: A numerical study. Int. J. Heat Mass Transf. **128**, 2019, 860-864.
64. Li, Y.; Gao, T.; Yang, Z.; Chen, C.; Luo, W.; Song, J.; Hitz, E.; Jia, C.; Zhou, Y.; Liu, B., et al., 3D-Printed, All-in-One Evaporator for High-Efficiency Solar Steam Generation under 1 Sun Illumination. Adv. Mater. **29**, 2017, 1700981.

Preprints (www.preprints.org) | NOT PEER-REVIEWED | Posted: 28 December 2023 doi:10.20944/preprints202312.2214.v1

65. Kashyap, V.; Ghasemi, H., Solar heat localization: concept and emerging applications. J. Mater. Chem. A. **8**, 2020, 7035-7065.
66. Li, D.; Cheng, Y.; Luo, Y.; Teng, Y.; Liu, Y.; Feng, L.; Wang, N.; Zhao, Y., Electrospun Nanofiber Materials for Photothermal Interfacial Evaporation. Materials. **16**, 2023, 5676.
67. Guan, W.; Guo, Y.; Yu, G., Carbon materials for solar water evaporation and desalination. Small. **17**, 2021, 2007176.
68. Elsheikh, A.H.; Sharshir, S.W.; Ali, M.K.A.; Shaibo, J.; Edreis, E.M.; Abdelhamid, T.; Du, C.; Haiou, Z., Thin film technology for solar steam generation: A new dawn. Sol. Energy. **177**, 2019, 561-575.
69. Wu, Z.; Sun, H.; Xu, Z.; Chi, H.; Li, X.; Wang, S.; Zhang, T.; Zhao, Y., Underwater Mechanically Tough, Elastic, Superhydrophilic Cellulose Nanofiber-Based Aerogels for Water-in-Oil Emulsion Separation and Solar Steam Generation. ACS Appl. Nano Mater. **4**, 2021, 8979-8989.
70. Zhang, Q.; Yang, H.; Xiao, X.; Wang, H.; Yan, L.; Shi, Z.; Chen, Y.; Xu, W.; Wang, X., A new self-desalting solar evaporation system based on a vertically oriented porous polyacrylonitrile foam. J. Mater. Chem. A. **7**, 2019, 14620-14628.
71. Fang, Q.; Li, T.; Lin, H.; Jiang, R.; Liu, F., Highly Efficient Solar Steam Generation from Activated Carbon Fiber Cloth with Matching Water Supply and Durable Fouling Resistance. ACS Appl. Energy Mater. **2**, 2019, 4354-4361.
72. Hao, D.; Yang, Y.; Xu, B.; Cai, Z., Efficient solar water vapor generation enabled by water-absorbing polypyrrole coated cotton fabric with enhanced heat localization. Appl. Therm. Eng. **141**, 2018, 406-412.
73. Wang, J.; Shi, Q.; Li, C.; Zhang, Y.; Du, S.; Mao, J.; Wang, J., Pistia-Inspired Photothermal Fabric based on Waste Carbon Fiber for Low-Cost Vapor Generation: An Industrialization Route. Adv. Funct. Mater. **32**, 2022, 2201922.
74. Li, E.; Pan, Y.; Wang, C.; Liu, C.; Shen, C.; Pan, C.; Liu, X., Asymmetric superhydrophobic textiles for electromagnetic interference shielding, photothermal conversion, and solar water evaporation. ACS Appl. Mater. Interfaces. **13**, 2021, 28996-29007.
75. Zhang, Q.; Xiao, X.; Zhao, G.; Yang, H.; Cheng, H.; Qu, L.; Xu, W.; Wang, X., An all-in-one and scalable carbon fibre-based evaporator by using the weaving craft for high-efficiency and stable solar desalination. J. Mater. Chem. A. **9**, 2021, 10945-10952.
76. Hu, N.; Xu, Y.; Liu, Z.; Liu, M.; Shao, X.; Wang, J., Double-layer cellulose hydrogel solar steam generation for high-efficiency desalination. Carbohydr. Polym. **243**, 2020, 116480.
77. Zha, X.-J.; Zhao, X.; Pu, J.-H.; Tang, L.-S.; Ke, K.; Bao, R.-Y.; Bai, L.; Liu, Z.-Y.; Yang, M.-B.; Yang, W., Flexible Anti-Biofouling MXene/Cellulose Fibrous Membrane for Sustainable Solar-Driven Water Purification. ACS Appl. Mater. Interfaces. **11**, 2019, 36589-36597.
78. Cheng, G.; Wang, X.; Liu, X.; He, Y.; Balakin, B.V., Enhanced interfacial solar steam generation with composite reduced graphene oxide membrane. Sol. Energy. **194**, 2019, 415-430.
79. Zhu, B.; Kou, H.; Liu, Z.; Wang, Z.; Macharia, D.K.; Zhu, M.; Wu, B.; Liu, X.; Chen, Z., Flexible and washable CNT-embedded PAN nonwoven fabrics for solar-enabled evaporation and desalination of seawater. ACS Appl. Mater. Interfaces. **11**, 2019, 35005-35014.
80. Cai, G.; Xu, Z.; Yang, M.; Tang, B.; Wang, X., Functionalization of cotton fabrics through thermal reduction of graphene oxide. Appl. Surf. Sci. **393**, 2017, 441-448.
81. He, M.; Dai, H.; Liu, H.; Cai, Q.; Liu, Y.; Wang, L.; Qin, X.; Yu, J., High-performance solar steam generator based on polypyrrole-coated fabric via 3D macro-and microstructure design. ACS Appl. Mater. Interfaces. **13**, 2021, 40664-40672.
82. Wang, J.; Wang, W.; Feng, L.; Yang, J.; Li, W.; Shi, J.; Lei, T.; Wang, C., A salt-free superhydrophilic metal-organic framework photothermal textile for portable and efficient solar evaporator. Sol. Energy Mater Sol. Cells. **231**, 2021, 111329.
83. Peng, H.; Wang, D.; Fu, S., Artificial transpiration with asymmetric photothermal textile for continuous solar-driven evaporation, spatial salt harvesting and electrokinetic power generation. J. Chem. Eng. **426**, 2021, 131818.
84. Gao, S.; Dong, X.; Huang, J.; Dong, J.; Maggio, F.D.; Wang, S.; Guo, F.; Zhu, T.; Chen, Z.; Lai, Y., Bioinspired Soot-Deposited Janus Fabrics for Sustainable Solar Steam Generation with Salt-Rejection. Global chall. **3**, 2019, 1800117.
85. Qin, Z.; Sun, H.; Tang, Y.; Yin, S.; Yang, L.; Xu, M.; Liu, Z., Bioinspired Hydrophilic-Hydrophobic Janus Composites for Highly Efficient Solar Steam Generation. ACS Appl. Mater. Interfaces. **13**, 2021, 19467-19475.
86. Wang, K.; Huo, B.; Liu, F.; Zheng, Y.; Zhang, M.; Cui, L.; Liu, J., In situ generation of carbonized polyaniline nanowires on thermally-treated and electrochemically-etched carbon fiber cloth for high efficient solar seawater desalination. Desalination. **481**, 2020, 114303.
87. Qi, P.; Ren, J.; Ling, S., Animal Silk-Derived Amorphous Carbon Fibers for Electricity Generation and Solar Steam Evaporation. Front. Chem. **9**, 2021.

Preprints (www.preprints.org) | NOT PEER-REVIEWED | Posted: 28 December 2023 doi:10.20944/preprints202312.2214.v1

88. Xiao, P.; Gu, J.; Zhang, C.; Ni, F.; Liang, Y.; He, J.; Zhang, L.; Ouyang, J.; Kuo, S.-W.; Chen, T., A scalable, low-cost and robust photo-thermal fabric with tunable and programmable 2D/3D structures towards environmentally adaptable liquid/solid-medium water extraction. Nano Energy. **65**, 2019, 104002.
89. Bai, W.; Zhang, X.; Chen, Y.; Lian, Z.; Zheng, S.; Chen, X.; Lin, Y.; Jian, R., Environmental-friendly biomass-based Janus ink/urushiol modified cotton fabric for efficient solar-driven interfacial evaporation. J. Chem. Eng. **476**, 2023, 146784.
90. Du, H.; Ge, C.; Xu, D.; Qian, Y.; Chen, Z.; Gao, C.; Song, B.; Shen, Z.; Chen, J.; Liu, K., et al., Multifunctional woven fabric for integrated solar-driven water generation and personal thermal management. Cellulose. **30**, 2023, 9207-9220.
91. Gao, C.; Zhou, B.; Li, J.; Chen, Y.; Wang, Q.; Mao, J.; Guo, J., Reversed vapor generation with Janus fabric evaporator and comprehensive thermal management for efficient interfacial solar distillation. J. Chem. Eng. **463**, 2023, 142002.
92. Wu, D.; Liang, J.; Zhang, D.; Zhang, C.; Zhu, H., Solar evaporation and electricity generation of porous carbonaceous membrane prepared by electrospinning and carbonization. Sol. Energy Mater. Sol. Cells. **215**, 2020, 110591.
93. Fan, X.; Lv, B.; Xu, Y.; Huang, H.; Yang, Y.; Wang, Y.; Xiao, J.; Song, C., Electrospun reduced graphene oxide/polyacrylonitrile membrane for high-performance solar evaporation. Solar Energy. **209**, 2020, 325-333.
94. Tessema, A.A.; Wu, C.-M.; Motora, K.G.; Naseem, S., Highly-efficient and salt-resistant CsxWO3@ g-C3N4/PVDF fiber membranes for interfacial water evaporation, desalination, and sewage treatment. Compos Sci Technol. **211**, 2021, 108865.
95. Ding, Q.; Guan, C.; Li, H.; Shi, M.; Yang, W.; Yan, H.; Zuo, X.; An, Y.; Ramakrishna, S.; Mohankumar, P., Solar-driven interfacial evaporation based on double-layer polylactic acid fibrous membranes loading Chinese ink nanoparticles. Solar Energy. **195**, 2020, 636-643.
96. Waisi, B.I.; Manickam, S.S.; Benes, N.E.; Nijmeijer, A.; McCutcheon, J.R., Activated Carbon Nanofiber Nonwovens: Improving Strength and Surface Area by Tuning Fabrication Procedure. Ind. Eng. Chem. Res. **58**, 2019, 4084-4089.
97. Liu, Y.; Liu, H.; Xiong, J.; Li, A.; Wang, R.; Wang, L.; Qin, X.; Yu, J., Bioinspired design of electrospun nanofiber based aerogel for efficient and cost-effective solar vapor generation. J. Chem. Eng. **427**, 2022, 131539.
98. Gao, T.; Li, Y.; Chen, C.; Yang, Z.; Kuang, Y.; Jia, C.; Song, J.; Hitz, E.M.; Liu, B.; Huang, H., et al., Architecting a Floatable, Durable, and Scalable Steam Generator:Hydrophobic/Hydrophilic Bifunctional Structure for Solar Evaporation Enhancement. Small Methods. **3**, 2019, 1800176.
99. Liu, H.; Liu, Y.; Wang, L.; Qin, X.; Yu, J., Nanofiber based origami evaporator for multifunctional and omnidirectional solar steam generation. Carbon. **177**, 2021, 199-206.
100. Qi, Q.; Wang, W.; Wang, Y.; Yu, D., Robust light-driven interfacial water evaporator by electrospinning SiO2/MWCNTs-COOH/PAN photothermal fiber membrane. Sep. Purif. Technol. **239**, 2020, 116595.
101. Liu, Y.; Xiong, J.; Li, A.; Wang, R.; Wang, L.; Qin, X., Plasmonic silver nanoparticle-decorated electrospun nanofiber membrane for interfacial solar vapor generation. Text. Res. J. **91**, 2021, 2624-2634.
102. Xu, W.; Hu, X.; Zhuang, S.; Wang, Y.; Li, X.; Zhou, L.; Zhu, S.; Zhu, J., Flexible and salt resistant Janus absorbers by electrospinning for stable and efficient solar desalination. Adv. Energy Mater. **8**, 2018, 1702884.
103. Zang, L.; Sun, L.; Zhang, S.; Finnerty, C.; Kim, A.; Ma, J.; Mi, B., Nanofibrous hydrogel-reduced graphene oxide membranes for effective solar-driven interfacial evaporation and desalination. J. Chem. Eng. **422**, 2021, 129998.
104. Wan, P.; Gu, X.; Ouyang, X.; Shi, S.; Deng, B.; Liu, J.; Chu, P.K.; Yu, X.-F., A versatile solar-powered vapor generating membrane for multi-media purification. Sep. Purif. Technol. **260**, 2021, 117952.
105. He, M.; Alam, M.K.; Liu, H.; Zheng, M.; Zhao, J.; Wang, L.; Liu, L.; Qin, X.; Yu, J., Textile waste derived cellulose based composite aerogel for efficient solar steam generation. Comp. Comm. **28**, 2021, 100936.
106. Mao, N.; Russell, S.J.; Pourdeyhimi, B., Chapter 12 - Characterisation, testing, and modelling of nonwoven fabrics, in Handbook of Nonwovens (Second Edition), S.J. Russell, Editor. 2022, Woodhead Publishing. p. 509-626.
107. Zhang, C.; Shi, Y.; Shi, L.; Li, H.; Li, R.; Hong, S.; Zhuo, S.; Zhang, T.; Wang, P., Designing a next generation solar crystallizer for real seawater brine treatment with zero liquid discharge. Nat. Commun. **12**, 2021, 998.
108. Zhang, C.; Xiao, P.; Ni, F.; Gu, J.; Chen, J.; Nie, Y.; Kuo, S.-W.; Chen, T., Breathable and superhydrophobic photothermic fabric enables efficient interface energy management via confined heating strategy for sustainable seawater evaporation. J. Chem. Eng. **428**, 2022, 131142.
109. Guo, Z.; Wang, G.; Ming, X.; Mei, T.; Wang, J.; Li, J.; Qian, J.; Wang, X., PEGylated Self-Growth MoS2 on a Cotton Cloth Substrate for High-Efficiency Solar Energy Utilization. ACS Appl. Mater. Interfaces. **10**, 2018, 24583-24589.

Preprints (www.preprints.org) | NOT PEER-REVIEWED | Posted: 28 December 2023 doi:10.20944/preprints202312.2214.v1

110. Liu, Z.; Wu, B.; Zhu, B.; Chen, Z.; Zhu, M.; Liu, X., Continuously Producing Watersteam and Concentrated Brine from Seawater by Hanging Photothermal Fabrics under Sunlight. Adv. Funct. Mater. **29**, 2019, 1905485.
111. Wang, H.; Yao, L.; Zhang, M.; Xu, R.; Ye, F.; Zhu, K.; Wang, H.; Zuo, H.; Ruan, F.; Feng, Q., In-Situ polymerized polypyrrole Janus cotton fabric for Solar-driven water evaporation in Textile-dying wastewater. Mater. Lett. **341**, 2023, 134299.
112. Zhang, H.; Ou, J.; Fang, X.; Lei, S.; Wang, F.; Li, C.; Li, W.; Hu, Y.; Amirfazli, A.; Wang, P., Robust superhydrophobic fabric via UV-accelerated atmospheric deposition of polydopamine and silver nanoparticles for solar evaporation and water/oil separation. J. Chem. Eng. **429**, 2022, 132539.
113. Irshad, M.S.; Wang, X.; Abbas, A.; Yu, F.; Li, J.; Wang, J.; Mei, T.; Qian, J.; Wu, S.; Javed, M.Q., Salt-resistant carbon dots modified solar steam system enhanced by chemical advection. Carbon. **176**, 2021, 313-326.
114. Chen, F.; Xu, L.; Tian, Y.; Caratenuto, A.; Liu, X.; Zheng, Y., Electrospun Polycaprolactone Nanofiber Composites with Embedded Carbon Nanotubes/Nanoparticles for Photothermal Absorption. ACS Appl. Nano Mater. **4**, 2021, 5230-5239.
115. Li, A.; Xiong, J.; Liu, Y.; Wang, L.; Qin, X.; Yu, J., Fiber-intercepting-particle structured MOF fabrics for simultaneous solar vapor generation and organic pollutant adsorption. J. Chem. Eng. **428**, 2022, 131365.
116. Yin, X.; Zhang, Y.; Xu, X.; Wang, Y., Bilayer fiber membrane electrospun from MOF derived Co3S4 and PAN for solar steam generation induced sea water desalination. J. Solid State Chem. **303**, 2021, 122423.

Disclaimer/Publisher's Note: The statements, opinions and data contained in all publications are solely those of the individual author(s) and contributor(s) and not of MDPI and/or the editor(s). MDPI and/or the editor(s) disclaim responsibility for any injury to people or property resulting from any ideas, methods, instructions or products referred to in the content.